

**OPTICAL SIGNAL TRANSMISSION IN NEW GENERATION FIBRES  
USING ADVANCED MODULATION FORMATS AND VCSEL  
TRANSMITER**

**BY**

**GEOFFREY KIPKOECH YEGON**

**A THESIS SUBMITTED IN PARTIAL OF FULFILMENT OF THE  
REQUIREMENTS FOR THE DEGREE OF DOCTOR OF PHILOSOPHY IN  
PHYSICS TO THE SCHOOL OF SCIENCE,  
UNIVERSITY OF ELDORET, KENYA**

**JANUARY, 2021**

## DECLARATION

### Declaration by the Candidate

This thesis is my original work and has not been presented for a degree in any other University. No part of this thesis may be reproduced without the prior written permission of the author and/or University Eldoret.

**GEOFFREY KIPKOECH YEGON**

Sign\_\_\_\_\_Date\_\_\_\_\_

**SC/PHD/P/035/12**

### Declaration by Supervisors

This thesis has been submitted for examination with our approval as University Supervisors.

Signature

\_\_\_\_\_Date\_\_\_\_\_

**DR. DAVID WASWA,**

University of Eldoret, Eldoret, Kenya

Signature

\_\_\_\_\_Date\_\_\_\_\_

**PROF. SAMWEL ROTICH,**

Moi University, Eldoret, Kenya



**DEDICATION**

To my beloved family

## ABSTRACT

In the current society, the data transmitted using the internet is tremendous and has been occasioned by the rapid broadening of communication infrastructure. The use of traditional NRZ format is becoming less applicable due to its bandwidth limitations. To address this bandwidth limitation there is need of advanced modulation formats that has high transmission capacity. A VCSEL transmitter was used because of its low operational cost occasioned by its low power. The work started with the implementation of the traditional Non Return to Zero (NRZ) modulation and phase shift keying (PSK) modulation systems as they form the basic building blocks in the design of higher modulation formats. Receiver sensitivity for 10 Gbps NRZ and PSK signals were obtained to be -18.60 dBm and -10.72 dBm respectively. NRZ gave a better receiver sensitivity of -7.88 dBm in comparison to PSK. A three level Pulse Amplitude Modulation (2-PAM) format was also implemented. However, due to high power requirement for 2-PAM, it could not be able to cross the BER threshold of  $10^{-9}$ . This makes it unsuitable for signal transmissions. A four level pulse amplitude modulation (4-PAM) that doubles the data rate per channel from 10 Gbps to 20 Gbps by transmitting more information in the amplitude of the carrier signal was implemented. In 4-PAM, two streams of electrical data each having a bit rate of 10 Gbps were combined so as to give a 20 Gbps multilevel system with a receiver sensitivity of -6.04dBm. However, 4-PAM had a higher penalty compared to NRZ and PSK. The possibility of using a single photodiode in demodulating the multilevel signal reduces the cost of implementing the scheme since no complex circuitry is required for both transmission and reception. Moreover, 4-PAM when integrated in a Dense Wavelength Division Multiplexing (DWDM) system will achieve even higher data rate per channel thus saving on the cost of capital investment and hence an efficient utilization of the available bandwidth. VCSEL and DFB lasers were also compared at transmission distance of 3.21 km. VCSEL showed very low sensitivity of -3.86 dBm as compared to -12.6 dBm for DFB. VCSEL being a low power laser has a low sensitivity. 4-PAM format therefore with VCSEL as a transmitter is suitable for implementing in access (Municipal) networks hence creating jobs by ensuring that businesses have fast, affordable and a very reliable Internet access. This will improve the productivity of existing businesses and attract new businesses to communities. By so doing, it also allows individuals to work from home more effectively and efficiently, Support the use of advanced healthcare and security systems and also it will strengthen long term social investments in the form of better-linked schools and libraries. This will eventually improve the economy of the country.

## TABLE OF CONTENTS

<b>DECLARATION</b> .....	ii
<b>DEDICATION</b> .....	iii
<b>ABSTRACT</b> .....	iv
<b>TABLE OF CONTENTS</b> .....	v
<b>LIST OF FIGURES</b> .....	viii
<b>LIST OF ABBREVIATIONS</b> .....	x
<b>ACKNOWLEDGEMENT</b> .....	xii
<b>CHAPTER ONE</b> .....	1
<b>INTRODUCTION</b> .....	1
1.1 Introduction.....	1
1.2 Problem statement.....	3
1.3 Justification.....	4
1.4 Objectives .....	5
<b>CHAPTER TWO</b> .....	7
<b>LITERATURE REVIEW</b> .....	7
2.1 Introduction.....	7
2.2 Characteristics of communication link .....	8
2.2.1 Channel Capacity .....	8
2.2.2 Channel bandwidth ( $\Delta f$ ).....	8
2.2.3 Spectral efficiency (S.E) .....	10
2.2.4 Receiver sensitivity .....	11
2.3 Optical transmitter .....	11
2.3.1 Modulator technologies.....	12
2.3.2 Internal modulation or directly modulated lasers.....	13
2.3.3 External modulation.....	14
2.3.4 Mach-Zender modulators (MZMs).....	15
2.4 Modulation formats.....	17
2.4.1 Intensity Modulation.....	19
2.4.2 Advanced modulation formats .....	19
2.4.3 Phase Modulation.....	20
2.4.4 QAM Modulation.....	20
2.4.5 Multilevel pulse amplitude modulation (PAM) format with digital signal processing .....	21

2.4.6	Pulse Amplitude Modulation (PAM).....	21
2.5	Polarization .....	22
2.5.1	Polarized Light.....	23
2.5.2	Jones and Stokes Formalism .....	25
2.6	Transmission impairments .....	27
2.6.1	Attenuation.....	28
2.6.2	Dispersions.....	30
2.6.3	Polarization Mode Dispersion (PMD) .....	31
2.6.4	Chromatic Dispersion in optical fibres .....	32
2.6.5	Dispersion compensating fibres .....	34
2.7	VCSEL (Vertical-Cavity Surface-Emitting Laser) Technology .....	36
2.7.1	VCSEL Structure .....	38
2.7.2	VCSEL characteristics .....	39
2.8	Digital signal processing.....	41
<b>CHAPTER THREE.....</b>		<b>43</b>
<b>METHODOLOGY .....</b>		<b>43</b>
3.1	Introduction.....	43
3.2	Experimental investigation of State of Polarization (SOP) in fibres .....	43
3.3	Vertical Cavity Surface Emitting Lasers .....	44
3.4	Signal transmission at different lengths.....	47
3.5	Transmission using Phase modulation format .....	48
3.6	Pulse Amplitude Modulation (PAM).....	49
3.6.1	2-Pulse Amplitude Modulation (2-PAM) format.....	49
3.6.2	Transmission using 4-Pulse Amplitude Modulation (4-PAM) format .....	51
<b>CHAPTER FOUR.....</b>		<b>53</b>
<b>RESULTS AND DISCUSSIONS.....</b>		<b>53</b>
4.1	State of Polarization in fibres.....	53
4.2	VCSEL biasing and tunability .....	54
4.3	VCSEL optimization for transmission.....	56
4.4	Effects of chromatic dispersion on transmission using 1550 nm VCSEL .....	57
4.5	Chromatic dispersion effects on the VCSEL based links .....	58
4.6	External Intensity Modulation and MZM biasing.....	59
4.7	VCSEL transmission at different lengths.....	60
4.8	Effects of changing the bit rate on VCSEL transmission .....	61

4.9	Transmission using Phase modulation (PM) .....	62
4.10	Pulse Amplitude Modulation (PAM).....	63
4.10.1	Transmission using 2-Pulse Amplitude Modulation (2-PAM) .....	63
4.10.2	Transmission using 4-Pulse Amplitude Modulation (4-PAM) .....	65
4.11	Comparison of transmission penalties for IM, Phase modulation, 2-PAM and 4-PAM .....	68
4.12	Comparison of DFB laser and VCSEL .....	69
<b>CHAPTER FIVE .....</b>		<b>70</b>
<b>CONCLUSIONS AND RECOMMENDATIONS.....</b>		<b>70</b>
5.1	<b>CONCLUSION .....</b>	<b>70</b>
5.2	<b>RECOMMENDATIONS.....</b>	<b>72</b>
<b>REFERENCES.....</b>		<b>73</b>
<b>APPENDICES .....</b>		<b>79</b>
<b>APPENDIX I: MATLAB ALGORITHM .....</b>		<b>79</b>
<b>APPENDIX II: SIMILARITY REPORT .....</b>		<b>81</b>

## LIST OF FIGURES

Figure 2.1 Internally modulated VCSEL laser.....	14
Figure 2. 2 Mach-Zender modulator structure .....	15
Figure 2. 3: Transfer function for the MZ modulator and operation condition for a NRZ modulation format.....	16
Figure 2. 4: Differential Group Delay(DGD) effects on (SSMF) (Zhang, 2012) .....	23
Figure 2. 5: Elliptically polarized light oriented at an angle relative to the x-axis with components $2E_{oy}$ and $2E_{ox}$ .....	24
Figure 2. 6: Representation of different states of polarization on the Poincaré sphere (Born & Wolf, 1999).....	27
Figure 2.7: Attenuation at different transmission windows .....	30
(O.F.S Furukawa Electric, 2018).....	30
Figure 2.8: Chromatic Dispersion in SMF.....	32
Figure 2. 9: Block diagram showing stages in compensation design .....	35
Figure 2. 10: Raycan VCSEL structure (Iga, 2000).....	39
Figure 2.11: Assembled VCSEL in a single driven connection mode.....	41
Figure 3.1: experimental set up block diagram of SOP in fibres .....	44
Figure 3.2: Polarization analyzer and a synchronous scrambler.....	44
Figure 3.3: Block diagram of experimental un-modulated Laser biasing.....	45
Figure 3.4: Experimental setup to investigate Chromatic dispersion effects on the VCSEL based links.....	46
Figure 3.5: External Intensity Modulation experimental setup using MZM.....	47
Figure 3.6: Experimental setup to demonstrate phase modulation .....	48
Figure 3.7: Experimental modulation setup for 2-PAM .....	50
Figure 3.8: 4-PAM Experimental modulation setup.....	51
Figure 4.1: Polarization states of (a) a stable SMF (b) disturbed SMF on a Poincare sphere. 53	53
Figure 4.2: SOP representation of (a) Stable PMF (b) disturbed PMF on a Poincare sphere.. 54	54
Figure 4.3: (a) 1310 nm VCSEL Un-modulated bias characteristics (b) 1310 nm VCSEL tunability .....	55
Figure 4.4: BER curves and eye diagrams at different bias currents for 1550 nm VCSEL at (a) 4.5 mA (b) 5.5 mA (c) 7.0 mA (d) 8.5 mA.....	56
Figure 4.5: Experimental demonstration of chromatic dispersion (a) eye diagram for B2B (b) eye diagram for 17 km G.652 fibre.....	57
Figure 4.6: Chromatic Dispersion effects on VCSEL based links (a) BER curves (b) B2B (c) 24.69 km G.655 SMF-RS fibre (d) 17 km G.652 fibre.....	58
Figure 4.7: Mach-Zender modulator biasing characteristics.....	59
Figure 4.8: BER graphs at different lengths for 10 Gbps .....	60
Figure 4.9: BER for B2B and 74.91 km transmission at 8.5 Gbps and 10 Gbps.....	61
Figure 4.10: BER and eye diagrams for PSK format.....	63
Figure 4.11: Arm P, Arm N and combined 2-PAM electrical signal.....	63
Figure 4.12: B2B electrical 10 Gbps 2-PAM eye diagram and its optical signal waveform ...	64
Figure 4.13: BER Graph for B2B and transmission of 3.21 km and their eye diagrams for 2-PAM at 15 Gbps .....	65

Figure 4.14: P, N and combined 4-PAM electrical data signal.....	66
Figure 4.15: B2B electrical 20 Gbps 4-PAM eye diagram .....	66
Figure 4.16 : PAM-4 signal BER curve and eye diagrams .....	67
Figure 4.17: BER curves for IM, Phase modulation, 2-PAM and 4-PAM .....	68
Figure 4.18: BER curves for DFB and VCSEL .....	69

**LIST OF ABBREVIATIONS**

ASE	Amplified Spontaneous Emission
CD	Chromatic Dispersion
CS-RZ	Carrier Suppressed Return to Zero
DCF	Dispersion-Compensating Fibre
DD	Direct-Detection
DGD	Differential Group Delay
DRA	Distributed Raman Amplification
DRS	Double Rayleigh Scattering
DSP	Digital Signal Processing
DWDM	Dense Wavelength Division Multiplexing
EDFA	Erbium-Doped Fibre Amplifiers
FDM	Frequency Division Multiplexing
FTTH	Fibre To The Home
FUT	Fibre Under Test
FWM	Four Wave Mixing
IM	Intensity-Modulation
ISI	Inter-Symbol Interference
NF	Noise Figure
NRZ	Non Return to Zero
NRZ-DPSK	Non Return to Zero Differential Phase Shift Keying
NRZ-OOK	Non Return to Zero On Off Keying
PAM	Pulse Amplitude Modulation
PCB	Printed Circuit Board



PIN	Positive-Intrinsic-Negative
PMD	Polarization Mode Dispersion
PMF	polarization maintaining fibre
PPG	Pattern Generator
PRBS	Pseudo-Random Bit Sequence
PSK	Phase Shift Keying
RIN	Relative Intensity Noise
RZ	Return to Zero
RZ-DPSK	Return to Zero Differential Phase Shift Keying
RZ-OOK	Return to Zero On Off Keying
SBS	Stimulated Brillouin Scattering
SMF	single mode fibre
SNR	Signal to Noise Ratio
SOP	state of polarization
SPM	Self Phase Modulation
SRS	Stimulated Raman Scattering
TDM	Time Division Multiplexing
VCSEL	Vertical Cavity Surface Emitting Laser
WDM	Wavelength Division Multiplexing
XPM	Cross Phase Modulation

## ACKNOWLEDGEMENT

Firstly, I would like to extend my sincere gratitude to my supervisors Dr. Waswa and Prof. Rotich whose guidance and many insights, concern and positive criticism have been so valuable throughout this journey. Thank you so much for your time, positive suggestions and all the assistances towards this work. I am also grateful to the Physics Department University of Eldoret (UOE) for according me this wonderful opportunity to undertake my PhD studies.

I sincerely acknowledge the research visit at Nelson Mandela University (NMU) that was funded under African Laser Centre (ALC) and NMU. Many thanks go to Prof. Tim Gibbon for the wonderful opportunity he accorded me. Thanks for making my dream a reality. I am deeply indebted to the members of optical fibre research unit group at NMU; Dr. George Isoe and Dr. Shukree Wassim, thanks for being there whenever I needed your assistance, I live to remember your valuable company.

To my family, saying thank you may not be enough but I hope that it conveys the message of my heart. Your precious time, prayers, sacrifice, inspiration, guidance and all kinds of support is sincerely appreciated. To my wife Noela, children Abigael, Leon, the late Debrah Chepchirchir and my dear parents Mr. and Mrs. Samwel Mutai thank you so much for your company and prayers.

To my colleagues and friends; Dr. Enoch, Dr. Boiyo, Arusei, Koech, Cherutoi and others, your help, suggestions, steadfast love, support and encouragement was very valuable. I appreciate each one's contribution in a special way. To each one of the above, I extend my deepest appreciation and your extreme generosity will be remembered always as the vessels God used for a noble purpose.

## **CHAPTER ONE**

### **INTRODUCTION**

#### **1.1 Introduction**

In the last two decades speedy growth of optical communication systems has been remarkable. Rapid growth of the optical communication systems in the past two decades has been remarkable. This has been necessitated by the ever growing demand for bandwidth. Commercial deployment of optical fibres started exclusively to serve long haul transmission systems. However, today optical fibre use has extended to access and metro networks. The high demand enhanced fibre manufacturing technologies, development in semiconductor lasers as well as optical detectors. Fibre to the home which has taken shape in parts of the world such as Asia, Europe, America and Fibre to the hut (FTTH) in some parts of Africa, Kenya included entails day to day businesses, academics and individual users relying on the high speed networks to undertake their daily activities. It encompasses among other things a variety of digital services such as internet, mobile television, mobile phones, fixed telephones, video conferencing and 3D entertainment. With this high demand, there has been a continuous research to come up with new technologies that meet the deliberate data rates.

Challenges that relate to capacity, sensitivity and implementation in telecommunication have been overcome using modulation and multiplexing techniques. Until recently, most Dense Wavelength Division Multiplexing (DWDM) systems within the C-band (1500-1550 nm) has been used to transmit 96 channels at 50 GHz channel spacing, conforming to the International Telecommunication Union (ITU) standards. In order to improve capacity and transmission distance, there is need to increase the spectral efficiency,

increase available bandwidth and reduce signal impairments accumulated per bits per symbol. Using techniques that transmit more bits per symbol spectral efficiency can be enhanced. (Koizumi *et. al.*, 2012 and Nakazawa *et. al.*, 2010) however, this can be restricted by noise and perhaps other distortions leading to reduction in sensitivity per bit. Due to complexity and cost of advanced techniques of pushing the transmission limit, impairment reduction and use of low noise amplifiers to reduce the noise levels are key to increasing transmission capacity as well as transmission distance in conventional methods (Karinou *et. al.*, 2015). Fibre-optic remains the most appropriate solution for meeting global communication needs due its near limitless capabilities, high speed and its bandwidth is huge (in terms of Tb/s). In addition it has low signal attenuation of approximately 0.2 dB/km, low signal distortion and low power requirement. Also it's immune to electromagnetic interference, non-conductive, non-radiative and non-inductive and cheap maintenance. The exponential rise in the clamour for high speed communication systems has imposed on networks to opt for higher bit rates. Therefore signals can be transmitted for longer distances without needing to be re-generated or amplified. However, as fibre optic cables costs much less to maintain, their initial cost of installation is high.

Despite these modern fibres having low attenuation of  $\leq 0.2dB/km$ , this value is still substantial enough to limit transmission reach. The attenuation problem was initially solved using optoelectronic repeaters in long haul systems (Tricker, 2002). Indeed, DWDM technique owes its success to the introduction of optical amplifiers and has resulted in increased capacity and span.

One of the most important elements in the system, which affects the choice of all other system parameters, is the optical modulation format. Signal optical spectral bandwidth, tolerance to chromatic dispersion, resistance to nonlinear crosstalk, susceptibility to accumulated noise, and other system performance measures are directly related to the optical modulation format. Non-return-to-zero had been the dominant optical modulation format in intensity-modulation, direct-detection (IM/DD) fibre-optic systems ( Agalliu & Lucki, 2014). Recent research in advanced optical modulation formats was motivated by the demand of high transmission capacity, better system reliability and optimum operation conditions. A variety of signal modulation formats have been studied extensively in telecommunication systems and networks (Kuchta, 2016). Although there is no modulation format that is immune to all the sources of performance degradations, a proper selection of an advanced optical modulation format does improve the system performance to some extent by minimizing degradation effect. The choice of optimum optical modulation format depends on many factors such as fibre types, per-channel data rate, wavelength spacing. In this work the performance of Non-Return to Zero (NRZ), Pulse Amplitude Modulation (PAM) and Phase Shift Keying (PSK) optical modulation formats have been demonstrated.

## **1.2 Problem statement**

Over the last decade the demand for bandwidth has been on the rise with increasing broadband access supporting data-intensive applications such as High Definition Television (HDTV), video on demand (VoD), telemedicine, 4G/5G network, online gaming, teleconferencing and virtual learning among others. These demands have put intense pressure on the communication infrastructures to provide broadband access

supporting diverse services. NRZ format and others have proved to have high receiver sensitivity but are becoming less applicable with increasing system capacity and transmission distance due to bandwidth limitations. Access network demand a lot of capacity and therefore NRZ and others are an impediment.

### **1.3 Justification**

Telecommunication in general is an enabler to achieving Vision 2030 and the “Big Four” agenda. The Ministry of Information, Communications and Technology (ICT) has the core responsibility for formulating, administering, managing and developing the Information, Broadcasting and Communication policy. To enhance the development of broadband, the Ministry of ICT in 2013, launched the National Broadband Strategy (NBS) aimed at transforming Kenya into a knowledge-based economy through the provision of quality broadband services to all citizens. The government of Kenya has also established ‘Huduma’ Centers in all the counties to ensure all Kenyans can access efficient Government services at their convenience. According to the Communications Authority of Kenya (CA), the sector’s regulator, availability of various technologies and services that offer faster and more reliable internet connections has continued to grow in the country with consumers embracing these services through access (municipal) networks. These networks create jobs by ensuring businesses have fast, affordable, and reliable Internet access. These networks will eventually improve the productivity of existing businesses and attract new businesses to communities, Allow individuals to work from home more effectively, Support advanced healthcare and security systems, and even Strengthen long term social investments in the form of better-connected schools and libraries. Moreover, the adoption of telemedicine and use of Artificial Intelligence (AI) in

medicine will ensure efficient and better utilization of resources and this will enhance universal health care coverage. The deployment of optical fibres which has become transmission medium of choice is meant to meet the high demand in communication throughput by finding innovative ways to increase the data carrying capacity of a single optical fibre and/or increase the bandwidth per channel. This increase in the network load requires a continuous increase in network capacity, improved spectrum efficiency and network management. In order to satisfy this current demand for bandwidth, higher modulation formats should be exploited together with relevant detection and performance evaluation techniques. In this work the devised higher order modulation technique (PAM) used can be suitably applied to the already deployed optical communication link by only modifying the transmitter without affecting the deployed fibre. Transmission of these multilevel signals could be implemented over the existing optical fibre communications infrastructure without significant alteration of the system architecture, thus saving the cost of capital investment and easing the system management and hence an efficient utilization of bandwidth. For the same available spectral region, this multilevel modulation scheme would offer a transmission capacity higher than its binary modulation counterparts. This work will go a long way to improve the economy of the country.

#### **1.4 Objectives**

The general objective of this work is to improve the transmission capacity for optical access networks.

The specific objectives are;

- ❖ To investigate the effects of dispersion in optical communication network

- ❖ To investigate NRZ, PSK, 2-PAM and 4-PAM with respect to sensitivity , capacity and data rates
- ❖ Compare VCSEL and DFB lasers using PAM for application in access networks
- ❖ To develop a Digital Signal Processing algorithm to demodulate the advanced modulation format (Phase and PAM) signals at the receiver



## CHAPTER TWO

### LITERATURE REVIEW

#### 2.1 Introduction

Basic optical communication system comprises of a transmitting device, the physical transmitting medium and a receiver. A transmitter transforms electrical signal to an optical signal. A transmission medium conveys the light signal from one point to another. The receiver on the other hand accepts and converts the light signal back to its electrical form. In transmitter section, a serial bit stream in electrical form is presented to a modulator, which superimposes the data appropriately onto the optical carrier for transmission over the fibre to the receiver.

At the receiver end, light is applied to a photo detector which converts the light signal from optical. The signal is then amplified and passed on to an analogue converter (ADC) circuit which isolates the individual state changes and their timing. It then decodes the sequence of state changes and reconstructs the original bit stream.

There are three main transmission modalities being used by the telecommunication industries, the copper wire, wireless and the optical fibre. Wireless technology which has greatly replaced copper wire in most sectors is still crucial in communication industry because of some of its conveniences such as mobility. However, optical fibre still stands as an enabler to wireless technology. The attraction of transmission over an optical fibre are mainly in its much larger capacity, immunity to electromagnetic interference and lower losses over long transmission reach compared to copper and wireless counterparts. At present, optical fibre transmission is seen as a dominant technology for both long haul

and short haul broadband data transmissions (Ju Han *et. al.*, 2005; Meltenisov & Matukhin, 2016).

## 2.2 Characteristics of communication link

### 2.2.1 Channel Capacity

The maximum rate at which data can be transferred through a communication link is called channel capacity (C). A channel is a passage used to send data from one or several transmitters to several or one receivers. A channel is measured by its bandwidth or data rate in bits/second and always has a certain capacity for transmitting data. The shift to using a multi-channel as opposed to using a single channel has significantly boosted the capacity of the current optical networks. WDM is a substantially utilized technology where multiple wavelengths are made use of to carry data simultaneously from several senders through the same fibre. (Elahmadi *et. al.*, 2009). The reliability and the bit rate of a communication system are mainly affected by the signal power, bandwidth and Signal-Noise-Ratio (SNR). (Dutton, 1998).

### 2.2.2 Channel bandwidth ( $\Delta f$ )

A range of frequencies which a channel can reliably transmit is called the bandwidth.. The Shannon sampling theorem says that, “if a channel has a bandwidth ( $\Delta f$ ) then the narrowest pulse that can be transmitted over the channel has duration”

$$t = \frac{1}{2\Delta f} . \quad (2.1)$$

Pulses that can be transmitted through the channel has a maximum rate given by  $C = 2\Delta f$  . In optical communication systems, a binary signal which carries one bit at a

time is normally considered for simplicity. Information is encoded on two amplitude levels for binary signals. However, it is possible to send data pulse with more than two levels using higher modulation formats. Multilevel signal pulses originates from a set of phases and /or state of polarization alphabets, amplitudes which will be used to send more bits per symbol.

If a multilevel transmission system with  $M = 2^m$  alphabets one could transmit at a channel capacity of (Dutton, 1998)

$$C = m \cdot 2 \cdot \Delta. = \log_2 M \cdot 2 \Delta. \quad (2.2)$$

where  $M$  represents the number of levels or symbols for a given number 'm' of arbitrary variables.

Equation (2.2) shows that channel capacity can be increased by simply adding the number of bits per symbol (m) or by expanding the bandwidth of the channel  $\Delta f$ . However in a real communication link, the number of bits per symbol must be limited. Channels may get distorted if high power is put and definitely nonlinearities will kick in. In a channel the number of levels is restricted by SNR. Theoretically, the best multilevel encoding that can be achieved for a signal with amplitude  $A_s$  and a noise signal of maximum amplitude

$A_N$  is given by (Dutton, 1998):

$$M = \frac{A_s}{A_N} \quad (2.3)$$

then the channel capacity translates to

$$C = m \cdot 2 \cdot \Delta. = \log_2 M \cdot 2 \Delta. = \Delta f \cdot 2 \log_2 M = \Delta f \cdot 2 \cdot \log_2 \frac{A_s}{A_N} \quad (2.4)$$

The main aim of having a communication system is to have a reliable link. A reliable system is one that achieves small error probabilities by using appropriate encoding and decoding schemes. Shannon in his theorem addressed the issue of the maximum rate at which information can be transmitted over a communications channel of a specified bandwidth in the presence of noise.

Shannon theory considers noise distribution as Gaussian. The channel capacity is therefore given by

$$C = 2 \cdot \Delta f \cdot \log_2 \left[ 1 + \frac{S}{N} \right] \quad (2.5)$$

where  $\frac{S}{N} = \frac{A_s}{A_N}$ . This is the ratio of the signal and noise power in the channel.

For a reliable communication the channel capacity depends on the noise power (N) and signal power (S) that it can accommodate. (Xia *et. al.*, 2007 and Lin *et. al.*, 2007). The symbol rate and not the bit rate determines the bandwidth required for communication. In digital communication systems, symbol rate is the number of waveform changes made to the transmission medium per unit time using a digitally modulated signal. The symbol rate is measured in baud (Bd) or symbol per second. In other words, symbol rate is the ratio of the bit rate to the number of bits transmitted per symbol whereas frequency of a system stream is called bit rate (Keiser, 2003 and Messerschmitt, 1999).

### 2.2.3 Spectral efficiency (S.E)

Spectral efficiency, information density refers to the information rate that can be transmitted over a given bandwidth ( $\Delta f$ ) in a specific communication link. The spectral efficiency is mathematically expressed as (Xia *et. al.*, 2007):

$$S.E = \frac{C}{\Delta f} = \log_2 \left[ 1 + \frac{S}{N} \right] \quad (2.6)$$

Measured in bits/second/Hz

But more often the bandwidth efficiency is expressed as:

$$S.E = \log_2 \left[ 1 + \frac{C.E_B}{N_0 \Delta f} \right] \quad (2.7)$$

Where  $S = C.E_B$ ,  $E_B$  =energy per bit and  $N_0$  =noise spectral density. From equation (2.7) total noise changes with the channel bandwidth .

#### 2.2.4 Receiver sensitivity

An important characteristic that indicate receiver performance in optical systems is the receiver sensitivity. This is the minimum received optical power for a given BER.. In telecommunications, standard BER of  $10^{-9}$  or below is used to define the receiver sensitivity. The bit error rate depends on the SNR which also depends on other various noise sources that distort the received optical signal. Amplified Spontaneous Emission, thermal noise and shot noise are significant noise contributors. Fibre dispersion can affect receiver sensitivity due to power penalties and depend on both fibre length and bit rate. The eye diagram can also be used to measure the performance of the receiver. Closing of the eye is linked to the corresponding rise in bit error rate. (Ibrahim, 2007).

#### 2.3 Optical transmitter

An optical transmitter is an optical communication component that comprises of a source and signal control electronics used to couple data onto optical carrier for transmission through the fibre. Semiconductor lasers that include, Distributed Feedback (DFB) lasers,

are intensively utilized laser sources since they conform well with optical fibre communication channel. (Agrawal, 2012 and Vodhanel *et. al.*, 1990). DFB lasers are also easy to modulate and are more power efficient. In the transmitter, the Radi Frequency (RF) electrical signal is modulated onto the light signal before injection into the fibre. Three basic modulation technologies namely direct/internal modulation (DM), electro-absorption modulation (EAM) and Mach-Zender modulation (MZM) are commonly employed to modulate the light signal in most optical communication systems. New and innovative ways of implementing these existing modulation technologies give rise to novel higher modulation formats. These modulation techniques are constantly being researched on with the need to solving the future requirements for high spectral efficiency and high bit rate dense wavelength division multiplexing (DWDM) optical networks (Jensen *et. al.*, 2013 and Lach & Idler, 2011). Another example of a semiconductor laser source is the Vertical Surface Emitting Laser (VCSEL). VCSELs are low power, wavelength tuneable, wavelength stable, compact in size, high bandwidth and are directly modulated. The capability of directly modulating the VCSEL using an input electrical signal reduces the complexity of requiring an additional external modulator. Moreover, the ability to adjust the transmission wavelength of Vertical Cavity Surface Emitting Lasers makes it also suitable for WDM systems.

### **2.3.1 Modulator technologies**

An optical modulator is a device that can be used to manipulate the intensity of the light signal. Three basic modulation technologies namely direct/internal modulation (DM), electro-absorption modulation (EAM) and Mach-Zender modulation are commonly employed to modulate the light signal in most optical communication systems. New and

innovative ways of implementing these existing modulation technologies give rise to novel higher modulation formats. Modulation techniques are constantly being researched on so as to come up with the solutions for future requirements of high bandwidth efficient and high bit rate dense wavelength division multiplexing (DWDM) optical networks.

### **2.3.2 Internal modulation or directly modulated lasers**

The simplest and cost effective method of converting electrical to optical signals is by using intensity modulation and directly modulated lasers with direct detection. The conversion is done within the laser while the detection happens in the photodiode. When the transmitted electrical signal is inscribed to the laser bias current, variation of the current that is driving the laser directly modulates the output power of the laser. When the optical signal reaches the photodiode, the intensity of the optical signal is converted back to an electrical signal based on the square-law detection of the PIN. For short reach applications directly modulated lasers such as VCSELs and DFB as in Figure 2.1 are usually preferred due to operational costs involved. (Pham & Monroy, 2012). However, DML signal quality is compromised. The compromised quality is due to strong modulations of electrical carriers within the laser that leads to some variation of carrier concentration in the laser active region that greatly affects the refractive index and in turn the frequency of a generated optical signal (Pham & Monroy, 2012). Thus, the internal laser modulation leads to undesired frequency chirping. The chirp of single frequency laser may be described by the adiabatic chirping coefficient that is proportional to the output laser power and the transient chirping which is proportional to logarithmic laser power as given in equation (2.8)

$$\Delta\nu(t) = \frac{\alpha}{4\pi} \cdot \frac{d}{dt} [\ln(P_L(t) + kP_L(t))] \quad (2.8)$$

Where  $\Delta\nu(t)$  is the instantaneous frequency deviation  $\alpha$  and it is also the line enhancement factor,  $k$  is the coefficient of adiabatic chirp and  $P_L$  is the laser output power (Krehlik, 2006 and Lach & Idler, 2011)

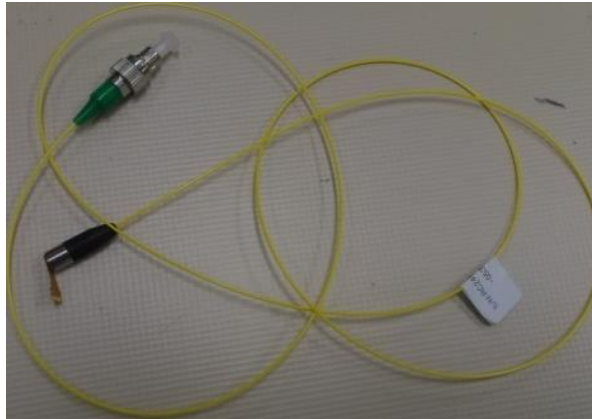


**Figure 2.1 Internally modulated VCSEL laser**

(Source: Author, 2017)

### 2.3.3 External modulation

The two types of external modulators available in optical communication are the Mach-Zender modulators and electro-absorption modulators. The external modulators usually have a higher bandwidth as compared to directly modulated lasers. Better quality of the signal can be achieved if there is independence between modulation and light generation. The integration of electro-absorption modulators in a laser substrate is possible because of their small nature (Yamamoto, 2012).



### 2.3.4 Mach-Zender modulators (MZMs)

A MZM is often used to control the phase and /amplitude of an optical signal. It works on the principle of interference. The incoming beam is split into two beams interferometer arms as shown in Figure (2.2).

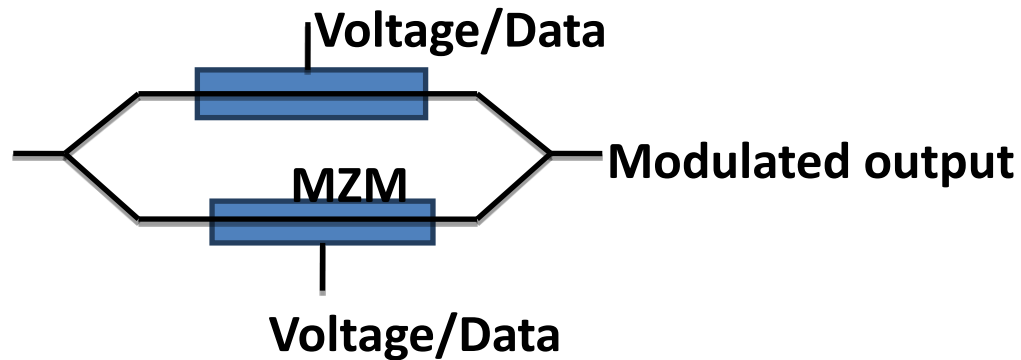


**Figure 2. 2 Mach-Zender modulator structure**

In one arm an external voltage is applied to an opto-electronic material such as Lithium Niobate that introduces a phase shift to the light signal passing through it. At the output coupler, the two signals will interfere constructively or destructively in response to voltage levels of the modulating signal.

The phase shift induced in the upper arm of the interferometer depends on the refractive index of the opto-electronic material, which itself depends on the applied external electric field. When a time dependent voltage  $v(t)$  is applied across the upper arm of the modulator, the refractive index will become time dependent and in turn the power transmission function  $[P_{out}/P_{in}]$  of the Mach-Zender interferometer will also be time dependent as shown in Figure 2.3.

Assuming equal power splitting and combining ratio of the couplers of the Mach-Zender interferometer, the power at the output depends on difference between the phase shifts

experienced by the light propagating in the upper and lower arm of the structure. Applied electrical voltage controls destructive or constructive interference, thereby producing intensity modulation and/or phase modulation. The power transfer function is given by

$$P_{out} = P_{in} \cos^2 \frac{\Delta\phi}{2} \quad (2.9)$$

Where  $\frac{\Delta\phi}{2}$  is the phase difference between the upper and the lower arm of the interferometer.

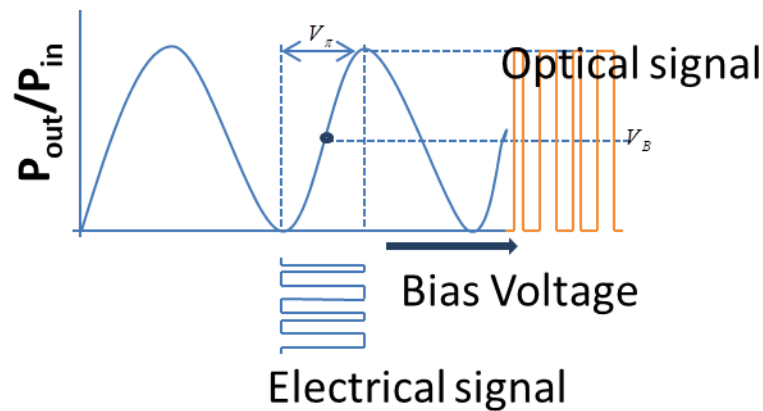


**Figure 2. 3: Transfer function for the MZ modulator and operation condition for a NRZ modulation format**

Due to their good modulation performance and possibility of independently modulating intensity and phase of the optical field, many advanced optical modulation formats are based on using these MZMs (Lauermann *et. al.*, 2014 and Peucheret & Fotonik, 2012a). They can be driven in different ways to generate a variety of important modulation formats. MZM produces a high quality signal, especially when the continuous wave signal from the laser is first guided into a preconditioning device such as a pulse carver modulator which is responsible for shaping the return to zero (RZ) pulses which are more robust to inter symbol interference (ISI) than their equivalent non return to zero (NRZ).

These kind of transmitters are almost uniquely used for ultra-long haul and high speed (40 Gbps and higher) communication systems (Winzer & Essiambre, 2006).

## **2.4 Modulation formats**

The bandwidth demand requires the use of higher modulation formats which are more spectral efficient compared to the traditional modulation formats. Therefore, the main aim in the design of an optical link is to investigate candidate optical modulation formats capable of achieving higher spectral efficiencies (SE) and eventually quality higher transmission capabilities at an affordable cost to meet the requirements of a particular network. Modulation is a technique by which the digital information is inscribed or superimposed onto an optical carrier and in its most general sense also includes coding to prevent transmission errors (Mohapatra *et. al.*, 2013 and Mohapatra *et. al.*, 2014). In optical communication systems, electromagnetic waves with frequencies of nearly 200THz are used to transfer information from one point to another (Al-Dwairi, 2013 and Mohapatra *et. al.*, 2014). An optical signal is fully characterized by its amplitude, frequency (wavelength), phase and its polarization state.

Amplitude Shift Keying (ASK) signal can be generated using either a directly modulated laser, an electro-absorption modulator or MZM (Lopez, 2013). Directly modulated lasers and electro-absorption modulators provide a cost effective solution and require less electrical power to drive the signals feeding the optical modulator compared to the MZM. However, the fact that they usually introduce some chirp into the signal makes them less suitable for long haul transmission.

ASK/IM is commonly used modulation format in the deployed optical transmission systems available today (Karinou *et. al.*, 2013 and Peucheret & Fotonik, 2012b). It is the

simplest digital modulation technique where digital information signal directly modulates the amplitude of an analogue optical carrier. Most optical communication systems used the binary ASK modulation format because it is simple and cost effective to implement. However, due to increase in demand for bandwidth, advanced modulation formats with improved performance compared to binary modulations are the potential candidates to meet the ever increasing communication demand (Abdullah & Talib, 2012; Haris, 2008 and Lopez, 2013).

In high speed DWDM systems, linear and nonlinear impairments become severe. Those linear impairments include chromatic dispersion (CD), and first order polarization mode dispersion (PMD); nonlinear impairments include self-phase modulation (SPM), cross-phase modulation (XPM) and four-wave mixing (FWM).

To combat both the linear and the nonlinear signal impairments in the transmission fibre, an optimal modulation format is desired. A modulation format with narrow optical spectrum can enable closer channel spacing and tolerate more CD distortion. In designing of an optical communication system, one needs to decide on how the electrical signal would be converted to optical stream. Two choices results in optical bit streams called RZ and NRZ. In RZ format, each optical pulse representing bit 1 is shorter than the bit slot and its amplitude returns to zero before bit duration is over while in NRZ format optical pulse remains on throughout the bit slot and its amplitude does not drop to zero (Lyubomirsky, 2005).

### 2.4.1 Intensity Modulation

The electric field associated with an optical signal can be written as  $E(t) = A_s \cos[w_0 t + \theta_s]$  ASK modulation format has the information encoded in the amplitude  $A_s$  of the optical field, while  $w_0$  and  $\theta_s$  are kept constants.

$E(t) = A(t) \cos[w_0 t + \theta_s]$  is most used format because of its simplicity. Depending whether a 1 or 0 bit is being transmitted,  $A_s$  takes one of the two fixed values during each bit period. When transmitting 0 bits,  $A_s$  is set to zero.

### 2.4.2 Advanced modulation formats

Most systems today use a binary amplitude modulation format with a pulse width equal to the time slot NRZ, since very simple and the cheapest transmitters and receivers can be used. The capacity of optical communication systems is rising exponentially in order to meet the rapidly increasing demand for data traffic. Limitations due to dispersion and nonlinearities in the optical fibre have become more stringent for higher bit rates. Most commercial systems use the NRZ modulation format (Dennis *et. al.*, 2003). However, there is an increasing effort in research being carried out to develop alternative modulation format (Dennis *et. al.*, 2003). Dispersion compensation is an essential part of any high-speed long-haul communication system (Jopson & Gnauck, 1995). The most commonly used dispersion compensation scheme is the Dispersion Compensation Fibres (DCF). For the next generation of optical communication systems to fulfill future capacity demands, state-of-the art dispersion management will be required to effectively compensate for dispersion in a wide bandwidth and minimize nonlinear signal degradation.

Higher order modulation formats are generally known as M-array modulation schemes since data can be encoded in the M possible alphabet symbols available to transmit the data. The data may be encoded on the amplitude, phase and/or frequency of the optical carrier signal. Every signal with  $M=2^m$  levels can encode a word of ‘m’ bits per symbol. Among advanced modulation formats are M-PAM, DQPSK and QAM which combines phase and amplitude. These advanced modulation formats can be used to improve the transmission performance and to achieve high spectral efficiency (Hoshida *et. al.*, 2002; Wuth *et. al.*, 2001). In this work four different modulation formats at bit rates of 10 Gbps per channel, were studied and their performances compared.

### 2.4.3 Phase Modulation

Phase Shift Keying (PSK) format has the optical bit stream generated by modulating the  $\theta_s$  phase while the amplitude  $A_s$  and the angular frequency  $\omega_0$  of the optical carrier kept constant.

$$E(t) = A_s \cos[\omega_0 t + \theta_s]$$

For M-ary PSK modulation, the angular aperture between constellation symbols is given by  $\frac{2\pi}{M}$ , where M is the number of symbols.

### 2.4.4 QAM Modulation

For amplitude and phase modulation, only one parameter of the optical signal was modified to produce a modulated signal. Hybrid modulation uses both amplitude and phase in a single modulation scheme. QAM modulation is obtained by modulating the phase and the amplitude of the electric field.

$$E(t) = A_s(t) \cos[\omega_0 t + \theta_s(t)] \quad (2.10)$$

Each constellation point is represented by a symbol made up of several bits. For  $n$  bits per symbol, the number of constellation points, or symbols, is  $M = 2^n$ . Therefore, for 16-QAM, the number of symbols is  $M = 2^4 = 16$ , where  $n = 4$ . By combining intensity and phase modulation, the number of phase states can be reduced for the same number of symbols, compared to M-PSK.

#### **2.4.5 Multilevel pulse amplitude modulation (PAM) format with digital signal processing**

The ever increasing demand for bandwidth requires the use of higher modulation formats which are more spectral efficient compared to the traditional formats. The generation and detection scheme for the higher modulation format will be explained in detail, with an evaluation of its performances based on experimental results.

#### **2.4.6 Pulse Amplitude Modulation (PAM)**

NRZ modulation is a traditional format where the signal is switched between two levels '0' and '1'. When more levels are introduced, it leads to a multilevel format with more levels assigned to the amplitude of the signal making it a more spectral efficient technique. Amplitude level is each assigned two bits of information. The number of levels the signal can have is determined by the number of bits transmitted per symbol. If a system with two bits ( $m=2$ ) per symbol it results in a 4-ASK signal. The quaternary signal is called 4-pulse amplitude modulation (4-PAM) or 4 level intensity modulation (4-IM) signals. The multilevel 4 PAM electrical signal was used to drive the internally/directly modulated VCSEL to generate 4-amplitude modulated optical signal.

Digital signal processing assisted receiver was developed and implemented to investigate the link performance through BER calculation for multilevel signal.

The developed 4-PAM optical communication system is a cost effective innovation for it uses both optical and electrical components operating at half the system bit rate compared to the bit rate of a traditional modulation format. A 20 Gbps optical communication system was developed from a  $2 \times 10$  Gbps.

## **2.5 Polarization**

Polarized light waves are light waves in which the vibrations occur in a single plane. The polarization state of the propagated wave is subject to unstable fluctuation when ambient conditions change only slightly (Okoshi, 1981). In an ideal Single Mode Fibre (SMF), light propagates in two polarization modes (fast and slow axis) with the same speeds. However, due to geometrical structure and random fibre imperfections in a real SMF, the optical pulses propagate at different speeds since an optical fibre has a random and varying refractive indices. This effect is known as birefringence and it causes a time delay between the fast axis and the slow axis. The propagation time delay is called Differential Group Delay (DGD), and results in pulse broadening and overlap. This phenomenon results in Polarization Mode Dispersion (PMD). For undisturbed transmission, the symmetrical and circularity of the core maintains the physical properties of the fibre. However, for disturbed fibre the symmetrical change in the states of polarization (SOPs) of the signal within the core is broken resulting in PMD. PMD induces error-bits due to the bit overlap and therefore degrades the signal during transmission as shown in Figure 2.4. PMD coefficient as a result of DGD due to intrinsic and extrinsic conditions is given by;



$$PMD = \frac{DGD}{\sqrt{L}} \quad (2.11)$$

Where PMD is the PMD coefficient and  $L$  is the length of the fibre (Ten & Edwards, 2006). PMD coefficient is expressed in  $ps/\sqrt{km}$

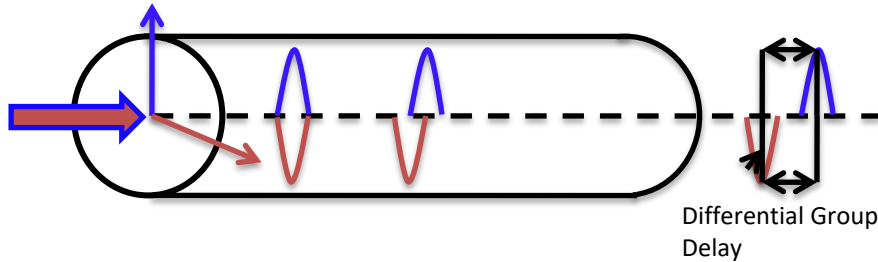


**Figure 2. 4: Differential Group Delay(DGD) effects on (SSMF) (Zhang, 2012)**

Polarization phenomena in optical fibres were observed in 1961 (Snitzer & Osterberg, 1961). It had emerged as a hurdle in the advancement of the modern light wave systems. Significance of polarization effect in optical fibres have been attributed to major developments on the system which include increasing bit rate and introduction of WDM channels in the fibre. Polarization effects have further been boosted by the introduction of optical amplifiers and increasing optical devices in the system.

### 2.5.1 Polarized Light

Polarization is a property of electromagnetic radiation describing the shape and the orientation of the electric field vector as a function of time or frequency, at a given point in space. If light is assumed to propagate in the positive  $z$ -direction, the real instantaneous electric field vectors along  $x$ -axis and  $y$ -axis can be written as (Zhang, 2012)

$$E(z,t) = E_x(z,t) + E_y(z,t) \quad (2.12)$$

Where,

$$E_x(z,t) = E_{ox} \cos(\omega t - kz + \delta_x) \quad (2.13)$$

$$E_y(z,t) = E_{oy} \cos(\omega t - kz + \delta_y) \quad (2.14)$$

where  $E_{ox}$  and  $E_{oy}$  are the amplitudes in the x and y-axis,  $k$  is the propagation constant,  $\omega$  is angular frequency,  $\delta$  is the phase angle of the electric field vectors, and  $t$  is time.

Therefore,

$$\left(\frac{E_x}{E_{ox}}\right)^2 + \left(\frac{E_y}{E_{oy}}\right)^2 - 2\frac{E_x}{E_{ox}}\frac{E_y}{E_{oy}}\cos\delta = \sin^2\delta \quad (2.15)$$

The trace of the state of polarization (SOP) is as shown in the Figure 2.5 and the angle  $\alpha$  is the SOP orientation angle relative to the x-axis.

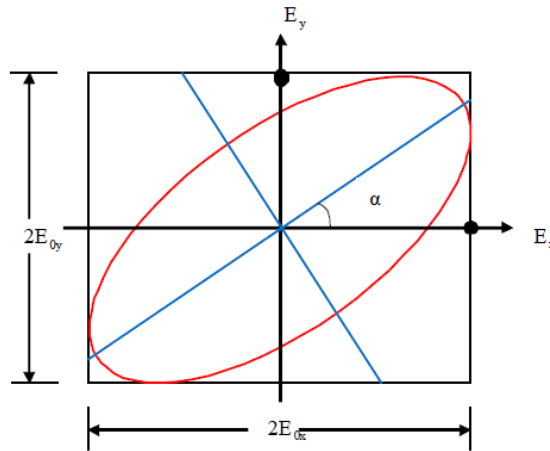


**Figure 2. 5: Elliptically polarized light oriented at an angle relative to the x-axis  
with components  $2E_{oy}$  and  $2E_{ox}$**

when the phase  $\delta = \pm n\pi$ ,  $n = 0, 1, 2, \dots$  the ellipse collapses into a straight line and it corresponds to a linearly polarized light with a constant orientation and varying amplitude. When  $\delta = \pm(2n+1)\frac{\pi}{2}$  ( $n = 0, 1, 2, \dots$ ), there is constant amplitude  $E_{ox} = E_{oy}$  but

varying orientation giving circularly polarized light. Elliptically polarized light has both varying orientation and amplitude.

### 2.5.2 Jones and Stokes Formalism

The state of polarization of a signal at any given frequency can be uniquely represented by two parameters. A Jones vector is essentially a  $2 \times 1$  unitary vector with complex components. Each complex component accounts for the magnitude and absolute phase of the electric field polarized in either the horizontal or vertical directions. The following equation represents the Jones vector (Al-Dwairi, 2013):

$$E = \begin{pmatrix} E_x \\ E_y \end{pmatrix} = \begin{pmatrix} E_{ox} e^{i\delta_x} \\ E_{oy} e^{i\delta_y} \end{pmatrix} \quad (2.16)$$

The use of Jones vectors to represent states of polarization provides a simple way of mathematically manipulating signals with a particular state of polarization. However, it becomes difficult to directly appreciate the changes in the state of polarization of a signal when the complex elements of a Jones vector change. In other words, Jones formalism can only deal with 100% polarization. However, in the general case, the propagating wave may consist of a polarized component and unpolarized component. Therefore, Stokes vector  $S = [S_0, S_1, S_2, S_3]$ , which offer a qualitative way of representing a state of polarization of a propagating light-wave is preferred. (Stokes 1852) introduced into optics the measurable or observables of polarization ellipse which are known as Stokes parameters (vectors). Stokes parameters can be derived by rewriting the amplitudes of equation (2.11) and (2.12) in terms of complex amplitudes. That is

$$\begin{aligned} E_x(t) &= E_{ox} \expj(\omega t + \delta_x) \\ E_y(t) &= E_{oy} \expj(\omega t + \delta_y) \end{aligned} \quad (2.17)$$

The term  $kz$  from equations (2.13) and (2.14) were dropped because only the time average of polarization ellipse (intensity) is of interest. The four parameters are given as (Stokes, 1852):

$$\begin{aligned}
 S_0 &= E_x E_x^* + E_y E_y^* = E_{ox}^2 + E_{oy}^2 \\
 S_1 &= E_x E_x^* - E_y E_y^* = E_{ox}^2 - E_{oy}^2 \\
 S_2 &= E_x E_y^* + E_y E_x^* = 2E_{ox} E_{oy} \cos\delta \\
 S_3 &= j(E_x E_y^* - E_y E_x^*) = 2E_{ox} E_{oy} \sin\delta
 \end{aligned} \tag{2.18}$$

The three normalized Stokes vectors  $S_1$ ,  $S_2$ , and  $S_3$  are coordinates on the Poincaré sphere that define the unique state of polarization; with  $S_1$  referring to vertical/horizontal polarizations,  $S_2$  to the  $+45^\circ$  or  $-45^\circ$  and  $S_3$  to right/left circular polarization. Linear polarizations are located on the equator; circular states are located at the poles with intermediate elliptical states continuously distributed between the equator and the poles as shown in Figure 2.6 below. Right-hand and left-hand elliptical states occupy the northern and southern hemispheres, respectively. Because a state of polarization is represented by a point, a continuous evolution of state of polarization can be represented as a continuous path on the Poincaré sphere.

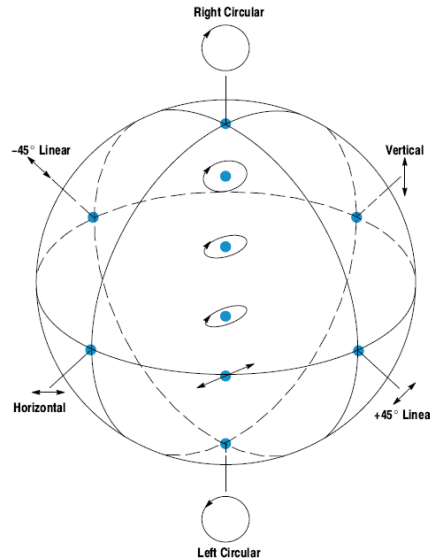


**Figure 2. 6: Representation of different states of polarization on the Poincaré sphere**  
(Born & Wolf, 1999)

The total intensity (polarized and un-polarized light),  $I_{tot} = S_0$ , while the intensity for polarized light  $I_{pol} = \sqrt{S_1^2 + S_2^2 + S_3^2}$ . The ratio of intensity of the polarized light to the total intensity gives a fundamental parameter in fibre optics known as degree of polarization (DOP) (Born, 1999), given as:

$$DOP = \frac{I_{pol}}{I_{tot}} = \frac{\sqrt{S_1^2 + S_2^2 + S_3^2}}{S_0}, 0 \leq DOP \leq 1 \quad (2.19)$$

If  $DOP=0$ , the light signal is not polarized and its Stokes vector will be found within the volume of the Poincaré sphere while if  $DOP=1$ , the light signal is completely polarized and the Stokes vector will be located on the surface of the unit sphere.

## 2.6 Transmission impairments

An optical fibre is often mistaken for a perfect transmission medium with almost limitless bandwidth, but in practice the propagation through an optical fibre is beset with several

limitations especially as distance is increased to multi-span amplified system. As the transmission systems evolved to longer distances and higher bit rates, the linear effects, which are attenuation and dispersion, become important factors. The degree to which fibre impairments are compensated for determines the transmission capacity of an optical fibre transmission system (Li *et. al.*, 2008).

### **2.6.1 Attenuation**

Efficient transmission of light at the operational wavelength(s) is the primary function of fibre optics needed for a range of applications (e.g. long-haul telecommunications, optical delivery for surgical or biomedical applications). Reduction in the intensity of light as it propagates within the fibre is called “attenuation”. The finite attenuation present in any optical fibre requires that fibre system design address degradation in signal strength through such approaches as signal amplification, interconnect optimization, fibre geometry design, and environmental isolation. An understanding of attenuation mechanisms and the potential for their minimization is, thus, of great importance in the efficient and economic use of fibre optics (Keiser, 2008).

Any process that results in a reduction in the light intensity measured after propagation through a material contributes to the observed optical attenuation. In principle, all attenuation mechanisms can be traced back to the multi-length scale structure of the glass itself (e.g. atomic structure, point defects, second-phase inclusions) or structures arising from the fiberization process and/or optical design of the fibre (e.g. interfacial structure at the core-clad interface, uniformity of core-clad structure along fibre length). Thus, the control of material structure (through composition, material processing, and fibre fabrication controls) is the primary means to reduce attenuation in the finished fibre. An

understanding, however, of the underlying optical phenomena at work and their relationship to material composition and structure is needed. The overall optical throughput (transmission) of an optical fibre can be quantified in terms of the input optical power,  $P(0)$ , and the output power,  $P(z)$  observed after light propagates a distance,  $z$ , along the fibre length given by the Beer's Law (Keiser, 2008)

$$p(z) = p(0)e^{-\alpha z} \quad (2.20)$$

where  $\alpha$  is the total attenuation coefficient (i.e. involving all contributions to attenuation). Beer's Law shows that transmitted power decreases exponentially with propagation distance through the fibre. In an optical fibre transmission, the attenuation coefficient is expressed as (Keiser, 2008);

$$\alpha \left( \frac{\text{dB}}{\text{km}} \right) = \frac{10}{z} \log_{10} \left[ \frac{p(0)}{p(z)} \right] = 4.34\alpha \cdot 34^{-1} \quad (2.21)$$

This final parameter is often referred to as the "fibre loss".

Multiple contributions to an overall transmission value arise from intrinsic fibre material properties as well as attenuation mechanisms associated with fibre fabrication. These different processes add to the observed reduction in transmitted power  $p(z)$  through contributions to the magnitude and wavelength dependence of  $\alpha$ .

Attenuation varies depending on the fibre type and the operating wavelength. For silica-based optical fibres, single-mode fibres have lower attenuation than multimode fibres. And generally speaking, the higher (or longer) the wavelength, the lower the attenuation as shown in Figure 2.7. This is true over the typical 800 - 1600 nm operating wavelength range for conventional datacom and telecom optical fibres. Single-mode fibres usually operate in the 1310 nm or 1550 nm regions, where attenuation is lowest. This makes

single-mode fibres the best choice for long distance communications. Multimode fibres operate primarily at 850 nm and sometimes at 1300 nm. Multimode fibres are designed for short distance use; the higher attenuation at 850 nm is offset by the use of more affordable optical sources (the lower the wavelength, the less expensive the optics) (OFS Furukawa Electric, 2007).

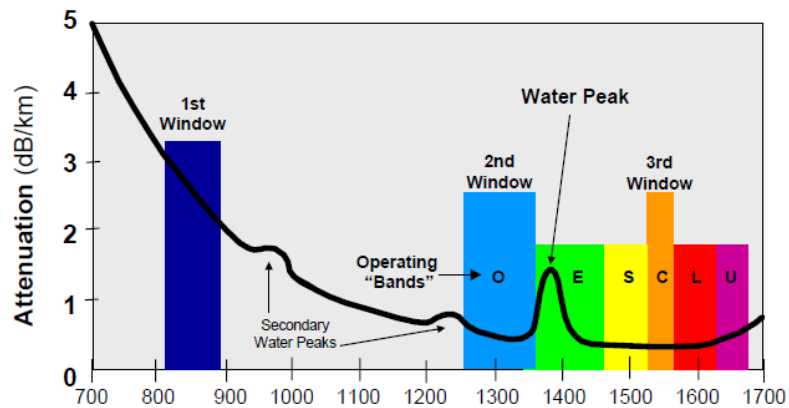


**Figure 2.7: Attenuation at different transmission windows**  
(O.F.S Furukawa Electric, 2018)

### 2.6.2 Dispersions

Single mode optical fibres have been exploited to their transmission limits. The limits of an optical fibre were not realized until its full implementation and greater transmission rates were passed through. Dispersion can be classified as two separate optical effects: chromatic dispersion and polarization mode dispersion (PMD) (Keiser, 2008).

Chromatic dispersion represents the fact that different wavelengths travel at different speeds, even within the same mode. Chromatic dispersion is the result of material dispersion and waveguide dispersion, or profile dispersion. PMD due to birefringence variation on the other hand can occur in single-mode optical fibres. SMFs support two



perpendicular polarizations of the original transmitted signal. If both polarization modes were perfectly round and free from all stresses, they would propagate at exactly the same speed, resulting in zero PMD. However, practical fibres are seldom perfect, thus the two perpendicular polarizations may travel at different speeds and, consequently, arrive at the end of the fibre at different times. Dispersion is a critical factor limiting the quality of signal transmission over optical links. Dispersion is a consequence of the physical properties of transmission medium. SMF, used in high speed optical networks, are subject to CD that causes pulse broadening depending on the wavelength and to PMD that causes pulse broadening depending on polarization. Excessive spreading causes bit to “overflow” their intended time slot and overlap adjacent bits. This will lead to the receiver having difficulty discerning and properly interpreting adjacent bits, increasing the BER (Keiser, 2008).

### **2.6.3 Polarization Mode Dispersion (PMD)**

Polarization mode dispersion (PMD) is a random effect resulting from intrinsic and extrinsic sources that causes the group velocity to vary with polarization state. Thus, over distance, a pulse will break up into multiple pulses, each with a specific polarization. This can severely constrain the bit rate-distance product of a system if left uncompensated. Intrinsic sources of PMD are minor imperfections resulting in noncircular fibre core geometry and residual stresses in the glass materials near the core region. Extrinsic sources of PMD include stress due to mechanical loading, bending, or twisting of the fibre and cable. Each of these sources induces a birefringence in the fibre, causing the otherwise degenerate polarizations of the fundamental mode to propagate at different speeds along the fibre and hence dispersing the optical pulse (Kaminow *et. al.*, 2010).The

fundamental mode is linearly polarized (LP) and is usually denoted as  $LP_{01}$ . It's easily assumed that the signal and the carrier maintain their state of polarization (SOP) inside the fibre. However, unless a special kind of polarization maintaining fibre is used, residual fluctuating birefringence of most fibres changes the SOP of any optical field in a random fashion leading to PMD, a phenomenon that has been studied extensively in recent years (Kaminow *et. al.*, 2010). Indeed, the effects of PMD have been observed in several experiments. The physical origin of PMD is essentially birefringence due to core eccentricity and ovalization.

#### 2.6.4 Chromatic Dispersion in optical fibres

Light within a medium travels at a slower speed than in a vacuum. The speed at which light travels is determined by the medium's refractive index. In an ideal situation, the refractive index would not depend on the wavelength of the light. Since this is not the case, different wavelengths travel at different speeds within an optical fibre as shown in Figure 2.8.

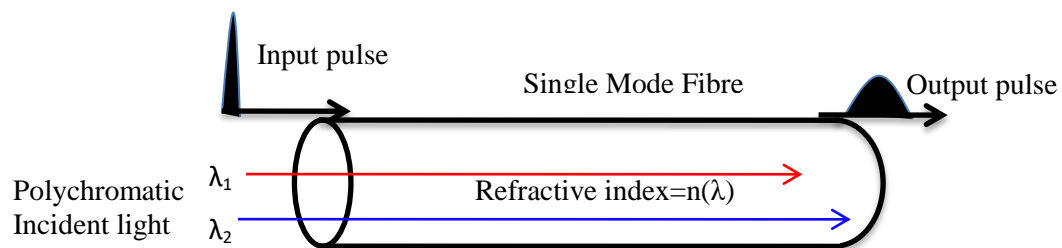


**Figure 2.8: Chromatic Dispersion in SMF**

Laser sources are spectrally thin, but not monochromatic. This means that the input pulse contains several wavelength components, traveling at different speeds, causing the pulse to spread. The detrimental effects of chromatic dispersion result in the slower wavelengths of one pulse intermixing with the faster wavelengths of an adjacent pulse,

causing inter-symbol interference. The chromatic dispersion of a fibre is expressed in ps/(nm.km), representing the differential delay, or time spreading (in ps), for a source with a spectral width of 1 nm traveling on 1 km of the fibre. It depends on the fibre type, and it limits the bit rate and the transmission distance.

As a consequence of its optical characteristics, chromatic dispersion of a fibre can be changed by varying one of the physical properties of the material. To reduce fibre dispersion, new types of fibre were invented, including dispersion-shifted fibres (ITU G.653) and non-zero dispersion-shifted fibre (ITU G.655). The most commonly deployed fibre in networks (ITU G.652), called “dispersion-un-shifted” single mode fibre, has a small chromatic dispersion in the optical window around 1310 nm, but exhibits a higher CD of 17ps/nm.km in the 1550 nm region. This dispersion limits the possible transmission length without compensation. ITU G.653 is a dispersion-shifted fibre (DSF), designed to minimize chromatic dispersion in the 1550 nm window with zero dispersion between 1525 nm and 1575 nm. But this type of fibre has several drawbacks, such as higher polarization mode dispersion than ITU G.652, and a high Four Wave Mixing risk, rendering DWDM practically impossible. For these reasons, another single mode fibre was developed: the Non-Zero Dispersion-Shifted Fibre (NZDSF). The ITU G.655 Non-Zero Dispersion-Shifted Fibres were developed to eliminate non-linear effects experienced on DSF fibres. They were developed especially for DWDM applications in the 1550 nm window. They have a cut-off wavelength around 1310 nm, limiting their operation around this wavelength.

### 2.6.5 Dispersion compensating fibres

The chromatic dispersion in fibre causes a pulse broadening and degrades the transmission quality, limiting the distance a digital signal can travel before needing regeneration or compensation. Fortunately, CD is quite stable, predictable, and controllable. Various methods allow for compensation of chromatic dispersion. CD comprises of the material and waveguide dispersion. Since material dispersion is constant, waveguide dispersion depends on the fibre geometrical parameters. The refractive index profile can be tailored so as to have a zero chromatic dispersion coefficient at the desired wavelength or have fibres with shifted dispersion characteristics such as Dispersion Shifted Fibres (DSF) or Standard Single Mode Fibres (SSMF). Moreover, Dispersion Compensation Fibre (DCF), with its large negative CD coefficient, can be inserted into the link at regular intervals to minimize its global chromatic dispersion. While each fibre spool of DCF adequately solves chromatic dispersion for one channel, this is not usually the case for all channels on a DWDM link. At the extreme wavelengths of a band, dispersion still accumulates and can be a significant problem. In this case, a tunable compensation module may be necessary at the receiver. CD can also be reduced by means of Bragg grating, but only for a narrow spectral region.

DCF was originally suggested (Lin *et. al.*, 1980) in the 1980s and is the most widely used technique for CD compensation in SMF. A schematic diagram illustrating how dispersion compensating fibre is applied within an optical telecommunication network is shown in Figure 2.9. To gain an understanding of how dispersion compensation is achieved within dispersion compensation fibre, consider an optical pulse propagating along standard single mode fibre whose group velocity  $V_g$  by (Agrawal, 2002)

$$V_g = \frac{dw}{d\beta} = \left( \frac{d\beta}{dw} \right)^{-1} \quad (2.22)$$

Since the zero dispersion wavelengths for standard single mode fibre is around 1310 nm and the central wavelength of the optical pulse is 1550 nm, the longer wavelength components within the pulse propagates slower than the shorter wavelength components.



**Figure 2. 9: Block diagram showing stages in compensation design**

After a certain time  $t$ , the optical pulse makes the transition from the conventional single mode fibre into the dispersion compensating fibre. The longer wavelength spectral components within the pulse propagate faster than the shorter wavelength spectral components. Consequently, it reduces the broadening and reshapes the optical pulse to its original form, unaffected by CD. DCF are manufactured in such a way to display very large negative CD coefficient values at 1550 nm, this is achieved by doping the fibre with very high quantities of  $\text{GeO}_2$ . Therefore, the cumulative positive dispersion incurred as the fibre length increases is cancelled by the large negative dispersion from the DCF. The typical dispersion coefficients for dispersion compensating fibres are  $-49 \text{ ps/nm.km}$  to  $-30 \text{ ps/nm.km}$  (Thorlabs, 2013). This allows for deployment of reduced lengths of dispersion compensating fibres, decreasing the total attenuation within an optical fibre communication system. Generally, dispersion compensating fibre displays extreme levels of attenuation  $\leq 0.265 \text{ dB/km}$  at 1550 nm window. Studies have shown that DCF has proven to be effective in reducing the CD within a high speed optical network system (Nuyts *et. al.*, 1997).

## 2.7 VCSEL (Vertical-Cavity Surface-Emitting Laser) Technology

VCSEL is a semiconductor-based laser diode. It emits a highly efficient optical beam vertically from its top surface. This type of lasers are a relatively recent type of semiconductor lasers and were invented in the mid-1980's. Light is emitted perpendicularly to the surface by lasing in a vertical cavity. Two highly reflective Distributed Bragg Reflectors (DBR) form a cavity. Forward biasing the pn-junction sandwiched between the two reflectors provides an optical gain. For short distance applications such as Ethernet, intra-system links and fibre channels, VCSELs have obtained honor as a superior technology. VCSELs have become a preferred technology for short datacom and local area networks significantly displacing edge-emitter lasers. (Gatto *et. al.*, 2009). This success was mainly due to a number of advantages of VCSELs which includes:

1. The VCSEL lasing wavelength is very stable, since it is fixed by the short Fabry-Perot cavity and can only operate within C-L bands.
2. Wavelength tunability makes it ideal for wavelength division multiplexing (WDM) (Koyama, 2006)
3. With improved Growth technology VCSEL cavity wavelength wafers are produced with less than a 2nm standard deviation. This allows for the fabrication of VCSEL 2-D arrays with little wavelength variation between the elements of the array. (Princeton optronics).
4. Sensitivity of emission wavelength to temperature variations in VCSELs is ~5 times less sensitive than in edge-emitters. The reason is that in VCSELs the refractive index

and physical thickness of the cavity have a weak dependence on temperature (Kondow *et. al.*, 2000).

5. Since VCSEL can be operated at temperatures upto 80°C, it does not require refrigeration and cooling system becomes very small, rugged and portable with this approach. (Lin *et. al.*, 2003 and Mereuta *et. al.*, 2004).

6. VCSELS provides  $\sim 1200 \text{ W/cm}^2$  and a near future projections of 2-4  $\text{kW/cm}^2$  as compared to edge-emitter with a maximum of about  $500 \text{ W/cm}^2$  this is because of gap between bar to bar which must be maintained for the flow of coolant. (Princeton optronics, 2008).

7. The VCSEL lasers through proper design of the cavity can emit in a single transverse mode which will greatly reduce the complexity and the cost of coupling optics and increasing the coupling efficiency to the fibre. (Princeton optronics, 2008).

8. VCSELS are not subject to catastrophic optical damage hence they are much more reliable than edge-emitters. (Princeton Optronics, 2008).

9. VCSELS have high manufacturing yields exceeding 90% (corresponds to  $\sim 5000$  high-power chips from a 2" wafer) while edge-emitters have low yields (edge-emitter 980 nm pump chip manufacturers typically only get  $\sim 500$  chips out of a 2" wafer). This is associated with complex manufacturing processes and reliability issues relating to catastrophic optical damage. .

10. VCSELS can be directly processed into monolithic 2-D arrays. However, this is not possible for edge-emitters.

11. VCSELs can be mounted in high power VCSEL 2-D arrays in a “junction-down” configuration. This makes the heat removal process very efficient as heat only traverses a few microns of AlGaAs material. (Koyama, 2006).
12. 2-D VCSEL arrays packaging is much easier than edge-emitters and hence significantly reduce the cost of high power modules. This is because VCSEL processing and heat sinking is much easier. (Koyama, 2006).

### **2.7.1 VCSEL Structure**

A gain medium of a VCSEL is an active region that is vertically stacked between two Distributed Bragg Reflectors (DBRs) as shown in Figure 2.10. VCSELs emit light directions normal to the surface of the active region layers; therefore amplification takes place in the cavity round trip. The length of the active region is minimized so as to achieve desired lasing wavelength. The generation of longitudinal modes associated to Fabry-Perot cavities is eliminated by the short cavity.

In order to provide enough gain, the active region of a VCSEL consisting of a number of quantum wells (QWs) interposed between higher band gap barriers and placed in an antinode of the optical field to achieve optimal gain. The optimal number and width of the central antinode of the optical number balances the increase in gain length and the reduction in the confinement factor with increased number of QWs thus limiting the number of QWs. DBR mirrors are highly reflective and oppositely doped i.e n-DBR and p-DBR. Through current-guiding structure, the active region of the VCSEL receives current by either proton injected surroundings or through an oxide aperture. There are different confinement schemes in VCSELs. These are the oxide confined, ion-implanted, etched air post, re-grown buried mesa, and the buried tunnel junction VCSEL structure.



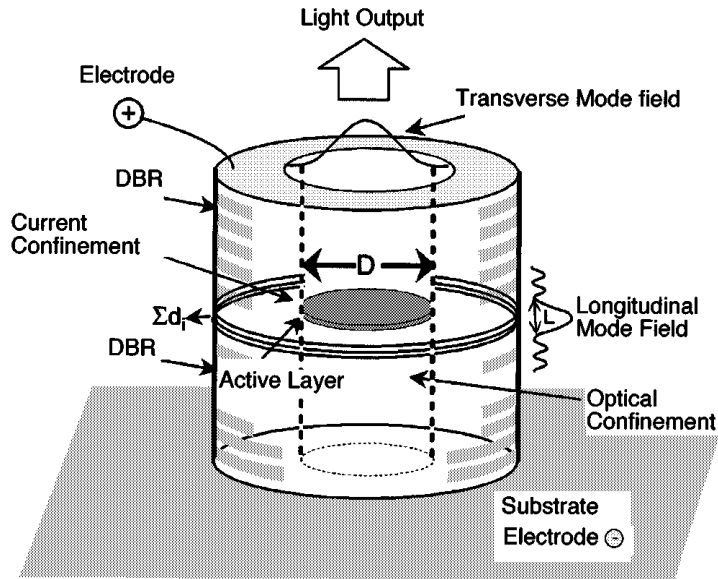


**Figure 2. 10: Raycan VCSEL structure (Iga, 2000)**

### 2.7.2 VCSEL characteristics

VCSEL used in experimental work were manufactured by the Raycan Company. The 1310 nm 10 Gbps and 1550 nm 10 Gbps were considered in this study. The possibility of having direct modulation in VCSEL is cost effective as opposed to using external modulation (Kipnoo *et. al.*, 2013). The VCSEL tenability to different channels can be done using bias current. Therefore, if VCSEL with similar characteristics are to be used, then each wavelength within the tenability range could be dedicated to each device. Wavelength division multiplexing which is normally used to increase the data rate over a single fibre in an array is necessitated by wavelength tunability and stability. Transmission at 1550 nm window is currently favored as it makes use of the minimum attenuation and its application in wavelength division multiplexing (WDM). Generally optical sources emitting at 1550 nm are suited for use on a G.655 fibre but it can be used on a G.652 fibre with penalty.

Frequency chirping and dispersion are two major defects experienced by VCSELs during normal operation (Petermann, 1988). Chirping is the instantaneous change of wavelength with varying optical powers. This results in time dependent instantaneous frequency changes. Dispersion dictates how the optical spectrum of a laser broadens during fibre transmission. A number of techniques for reducing and limiting chirping include injection locking (Bo *et. al.*, 2008) and filter off (Gibbon *et. al.*, 2011) setting to narrow the spectrum. The relationship between chirping and optical power is expressed as

$$\Delta\nu(t) = -\frac{\alpha}{4\pi} \left( \frac{d}{dt} \ln p(t) + kp(t) \right) \quad (2.23)$$

Where the time derivative of power (P) represents the transient chirp, the next part is adiabatic chirp due to instantaneous optical power,  $\alpha$  is the line enhancement factor and k is related to the geometry of the device and its non-linear gain.

The material composition are InAlGaAs, InGaAs and InAlAs which offers the VCSEL high reliability, reflectivity, low loss current confinement, reduced thermal impedance and low series resistance for long wavelength emissions (Kent *et. al.*, 2012). VCSEL emission wavelength can be adjusted by varying their bias currents. The VCSEL, bias and electrical radio frequency (RF) input signal are as shown in Figure 2.11.

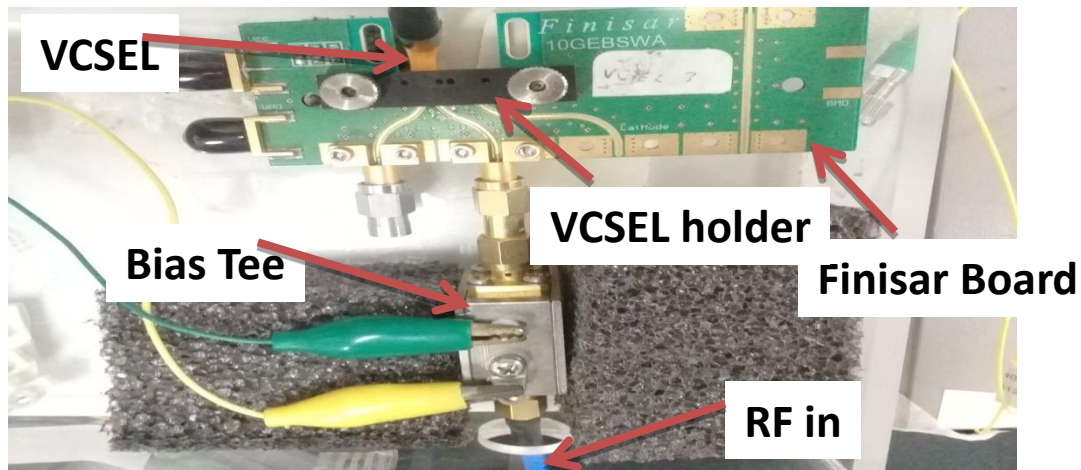


**Figure 2.11: Assembled VCSEL in a single driven connection mode**

(Source: Author, 2017)

The assembly consists of Printed Circuit Board (PCB) that is used to mount the VCSEL and also enables the connection of an external thermoelectric controller to control the temperature of the VCSEL cavity during operation. The  $50 \Omega$  termination is used to enable the VCSEL for single drive only.

## 2.8 Digital signal processing

The quality factor method is a system of evaluating the performance of a system where the noise distribution is assumed to be a Gaussian distribution. (Chagnon *et. al.*, 2014). In fibre optic communication, the receiver receives and demodulates the signal by comparing sampled voltage  $v(t)$  to a reference voltage known as the optimum decision threshold. It's usually assumed that the additive white Gaussian noise is the dominant cause of erroneous decisions and that the statistical probability of such a decision being made can be determined. For probability error to be determined, the probability density function for '0' and '1' levels must be known. This determines whether a signal will fall below or above the decision threshold. The probability density function can be described equation (2.24) by (Ratio, 2008)

$$\text{PROB}[v(t), \sigma_x] = \frac{1}{\sqrt{2\pi\sigma_x^2}} e^{-\frac{1}{2}\left(\frac{v(t)-v_s}{\sigma_x}\right)^2} \quad 2.24$$

Where  $v_s$  is the mean value of the density function,  $v(t)$  is the sampled voltage value at the receiver at time  $t$ , and  $\sigma$  is the standard deviation of the noise. To determine the BER, the standard deviation of the noise for zero level  $\sigma_L$  and one level  $\sigma_H$  and the voltage difference between the '0' level  $V_L$  and '1' level  $V_H$ . optical-signal-noise-ratio which describes the Q-factor is expressed as

$$Q_{(1,0)} = \frac{V_H - V_{TH}}{\sigma_H} = \frac{V_{TH} - V_L}{\sigma_L} \quad 2.25$$

The Q-factor can be described from equation (2.25) as

$$Q = \frac{V_H - V_L}{\sigma_H + \sigma_L} \quad 2.26$$

4-PAM since it has four levels, threshold for each of the levels must be determined with their respective standard deviations computed.. Three signal levels are practically applicable for 4-PAM format. Mean peak to peak voltage for each of the three eyes for level zero and one are calculated and their corresponding standard deviations determined. For each eye the threshold levels are then estimated based on their mean and standard deviations. The Q-factor is then calculated using the already obtained mean peak to peak voltages and their standard deviations. (Isoe *et. al.*, 2017). Finally, the actual BER is obtained as the cumulative error rate measurements done on each individual threshold values as indicated in equations (2.27) and (2.28). (Chabata *et. al.*, 2016)

$$\text{BER}_{4\text{-PAM}} = \text{BER}_1 + \text{BER}_2 + \text{BER}_3 \quad 2.27$$

$$= \frac{1}{2} \text{erfc} \left[ \frac{\mu_1 - \mu_0}{\sqrt{2}(\sigma_1 + \sigma_0)} \right] + \frac{1}{2} \text{erfc} \left[ \frac{\mu_2 - \mu_1}{\sqrt{2}(\sigma_2 + \sigma_1)} \right] + \frac{1}{2} \text{erfc} \left[ \frac{\mu_3 - \mu_2}{\sqrt{2}(\sigma_3 + \sigma_2)} \right] \quad 2.28$$

## **CHAPTER THREE**

### **METHODOLOGY**

#### **3.1 Introduction**

The chapter gives an account of the methods used in this work. The first section describes effects of polarization under different conditions. In the following section, it describes VCSEL transmission on different types of fibres and different bit rates. The optical link was evaluated through BER measurements and their corresponding eye diagrams. In the last section are the PSK and PAM formats experimental setups.

#### **3.2 Experimental investigation of State of Polarization (SOP) in fibres**

In the Figure 3.1, a WDM PRO 8000 DFB laser source from ThorLabs was used to generate the signal. The signal was then scrambled using A 3200 Synchronous scrambler from Adaptif photonics before monitoring the polarization using A 1000 polarization analyzer for a short period of time. Two types of fibres were used in this study; a Single Mode Fibre (SMF) and a Polarization Maintaining Fibre (PMF). The data for both the SMF and PMF were then collected under scrambled conditions. Another experiment was also performed both for SMF and PMF but under stable condition without the scrambler. SMF/PMF was fixed for a stable condition and the polarization monitored for a short period of time.

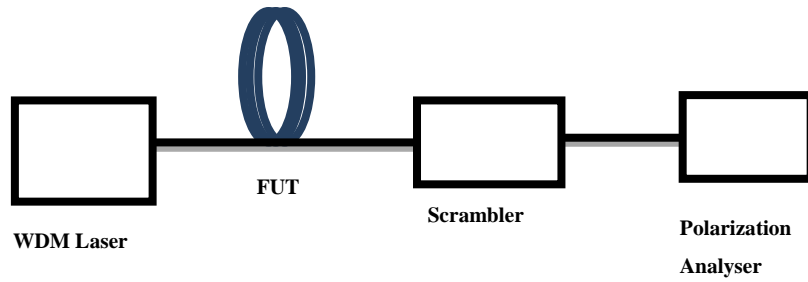


**Figure 3.1: experimental set up block diagram of SOP in fibres**

The Figure 3.2 shows the polarization analyzer and the synchronous scrambler from Adaptif Photonics used in the experimental work.



**Figure 3.2: Polarization analyzer and a synchronous scrambler**

(Source: Author, 2017)

### 3.3 Vertical Cavity Surface Emitting Lasers

#### 3.3.1 VCSEL biasing and tunability

VCSEL 1310 nm from Raycan was used in the experimentation. To reduce the chirp effects while maintaining good extinction ratio proper modulation depths should be maintained. The biasing and the ability to tune the emission wavelength of a VCSEL was

experimentally investigated and the setup is as shown in Figure 3.3. It was necessary to optimize the VCSEL so as to achieve good signal quality. The bias current was varied from 0 mA to 9.90 mA as the output power is measured using a power meter.

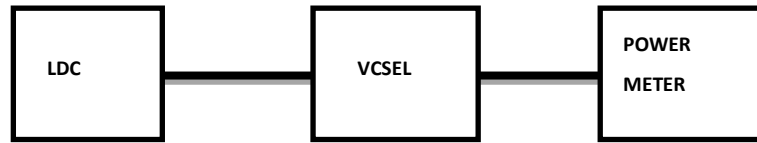


**Figure 3.3: Block diagram of experimental un-modulated Laser biasing**

### **3.3.2 Experimental investigation of effects of chromatic dispersion on high speed VCSEL transmission**

Transmission capabilities of 10 Gbps 1550 nm VCSEL are presented. This was done to investigate transmission capabilities of the VCSEL within the 1550 nm transmission windows. The experimental demonstration of direct modulation and detection was performed and is illustrated with the setup shown Figure 3.4. Using the laser diode controller the VCSEL was biased by varying the current and directly modulated with the 8.5-11.3 Gbps NRZ PRBS ( $2^7-1$ ) from a PPG via a Bias-Tee (BT). The VCSEL was biased above the threshold current at 5.5 mA. Modulated signal from the VCSEL was then conveyed through the fibre.. In this experiment, the FUT comprised of different types of fibre with varying lengths of a 17km G.652 and 24.69 km of a G.655. To vary the optical power going into the photodiode to imitate the loses in a fibre link, a variable optical attenuator was used.

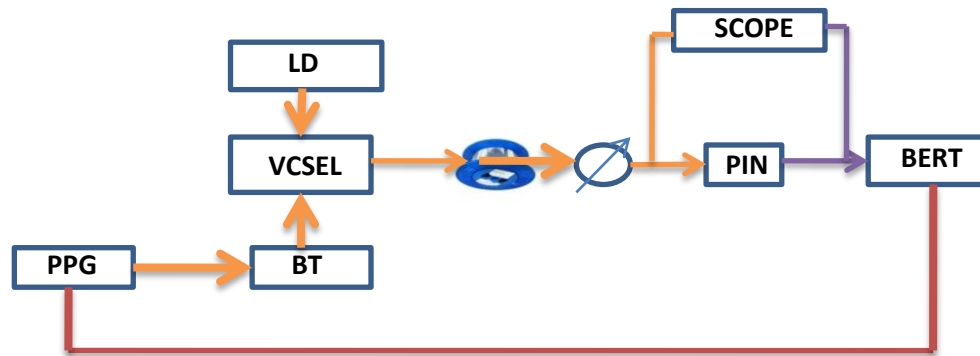


**Figure 3.4: Experimental setup to investigate Chromatic dispersion effects on the VCSEL based links**

The receiver consisted of PIN and an electrical amplifier (EA). For a signal to be detected by the BERT it needs to be amplified using EA. The quality of the transmitted signal was then evaluated by using the scope to plot the eye diagrams and BERT to measure BER. A clock signal from the Pattern Generator (PPG) was used to synchronize the 8.5-11.3 Gbps transmitted and received data signals. The quality of the signal was then finally characterized by analyzing the electrical data patterns, eye diagrams and BER measurements.

The modulation voltage is carefully varied as the BER of the transmission output is measured. The BER measurements were performed without the fibre (B2B) and through 24.69 km G.655 fibre link using a 1550 nm 10 Gbps VCSEL at 5.5 mA bias current.

For the second setup, BER measurements were performed for a B2B and 17 km G.652 fibre link using a 1550 nm 10 Gbps VCSEL at 5.5 mA. The tolerance to the effects of dispersion were measured for different types of fibres at different lengths. The optical link was evaluated through BER measurements for B2B, 24.69 km SMF-RS and 17 km



of G.652 fibre. CD coefficient are 4.5 ps/nm.km for G.655 fibre and 17ps/nm.km for G.652 at 1550 nm transmission window.

### 3.4 Signal transmission at different lengths

In Figure 3.5 the CW laser operating at 1550 nm was utilized. Pseudorandom bit sequence (PRBS) generator was used to modulate a NRZ pulse generator which operate as a laser driver. The laser was then connected to the MZM via Polarization Coupler (PC) which was then connected to the SMF.

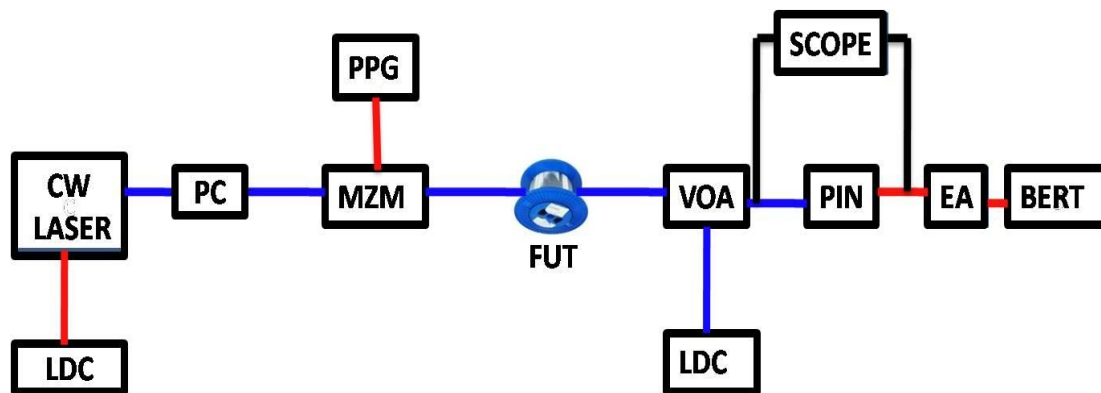


**Figure 3.5: External Intensity Modulation experimental setup using MZM**

The modulated signal was then transmitted through the fibre. Different fibre-links used were The eye diagram for B2B, transmission over 24.69 km SRS, 49.42 km (24.69 km SRS +24.73 km RS) and 74.91 km (24.69 km SRS +24.73 km RS+25.49 km SRS) SMF were collected with their corresponding BER curves. G.655 fibres had dispersion coefficients of 4.5 ps/(nm.km) at the 1550 nm transmission window while G.652 has dispersion coefficient of 17ps/nm.km. The fibre output was then connected to a VOA which varies the optical power to mimic typical power loss in a fibre link. The output was then fed to PIN Photodiode receiver having an error-free sensitivity of ~19 dBm for 8.5

Gbps and 10 Gbps at  $10^{-9}$  BER threshold. The output optical power was then varied so as to establish bit errors at different output power levels.

The electrical output from the PIN was then connected to EA to boost the signal so as to satisfy BERT operation voltage. A data recovery was then done at the end of the communication channel so as to measure the quality of the link. This was done by the measure of eye diagram and BER.

### 3.5 Transmission using Phase modulation format

The set up in Figure 3.6 is a complete optical transmission link demonstrating phase modulation. It comprises of a transmitter, fibre and a receiver.

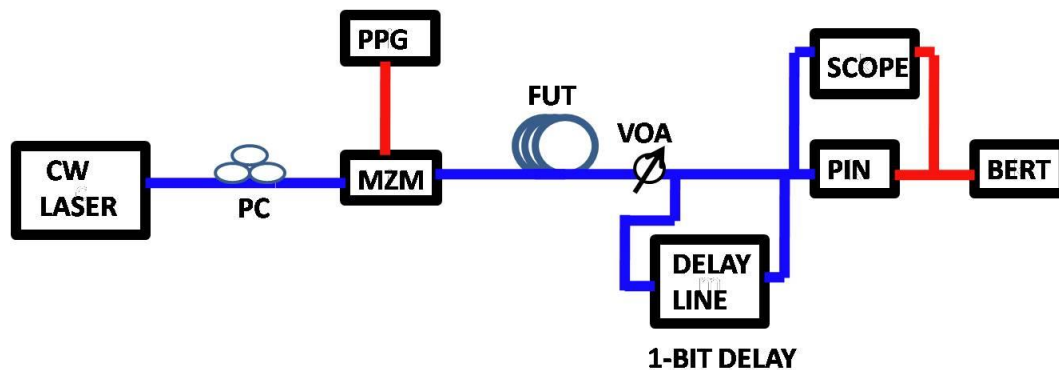


**Figure 3.6: Experimental setup to demonstrate phase modulation**

The PPG generate the PRBS ( $2^7-1$ ) which is then fed into one arm of the MZM. A continuous wave laser (WDM laser) at 1550 nm was linked to a Polarization Coupler (PC) before being fed into a MZM for phase modulation. In the MZM the incoming waveguide is split into two waveguide interferometer arms. In one arm an external voltage is applied to an opto-electronic material that introduces a shift in the phase to the light signal going through it. The phase shift experienced by light propagating on the two

arms is determined by the difference in the output power thereby producing a phase modulation.

The modulated signal from the MZM was then conveyed over the fibre. In this experiment, FUT comprised of 25.5 km of SRS fibre. To mimic the typical losses in a fibre, a VOA was used. The output was fed through a delay line (1 bit delay of 100 ps). The delay line converts a phase PSK signal into an intensity keyed signal. In the delay arm the signal is delayed by 100 ps which is equivalent to 1-bit period delay. The beams are then combined using a power combiner, and the two beams interfere either constructively or destructively. The signal is then connected to an optical receiver, PIN Photodiode with receiver sensitivity of  $\sim 19 \pm 1$  dBm at  $10^{-9}$  BER threshold. The output optical power was then varied so as to establish bit errors at different power levels. The electrical input of the receiver is connected to the sequence generator and the binary input connected to the PRBS output. This will enable the receiver to compare the transmitted and the received signal for the purpose of BER analysis.

### **3.6 Pulse Amplitude Modulation (PAM)**

#### **3.6.1 2-Pulse Amplitude Modulation (2-PAM) format**

The set up in Figure 3.7 shows a transmission link of a 2-PAM comprising a transmitter, optical transmission medium and the receiver.

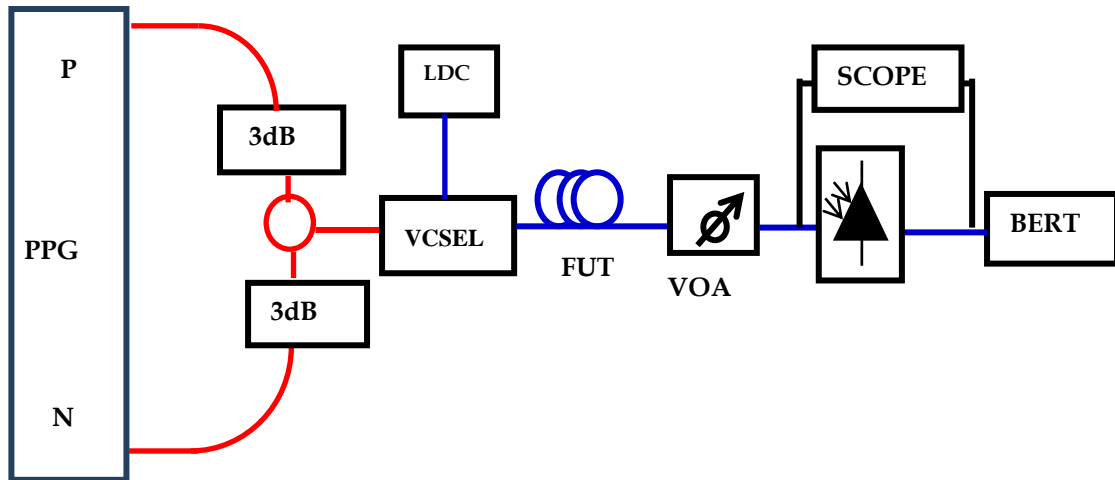


**Figure 3.7: Experimental modulation setup for 2-PAM**

The data output from the two arms (P and N) of a PPG generates the PRBS ( $2^7-1$ ) at 10 Gbps. After combining these data signals it directly modulates the VCSEL. The data output from arm P and N were both attenuated at 3dBm and had their electrical data sequence delayed in time by an integer multiple of a bit period hence de-correlating the two complemented bit sequences. When the two signal are combined in the power combiner, the two signal interfere constructively and destructively to produce a two level data signal (2-PAM). The signal is then transmitted through G.652 over a distance of 3.21 km. The optical signal power through the PIN was attenuated using a VOA so as to mimic the typical losses in the link.

The electrical input of the receiver is connected to the sequence generator and the binary input connected to the PRBS output. This will enable the receiver to compare the transmitted and the received signal for the purpose of BER analysis. The analysis were then done for B2B and 3.21 km through their eye diagrams and BER curves.

### 3.6.2 Transmission using 4-Pulse Amplitude Modulation (4-PAM) format

The set up in Figure 3.8 shows a transmission link of a 4-PAM comprising a transmitter, optical transmission medium and the receiver.

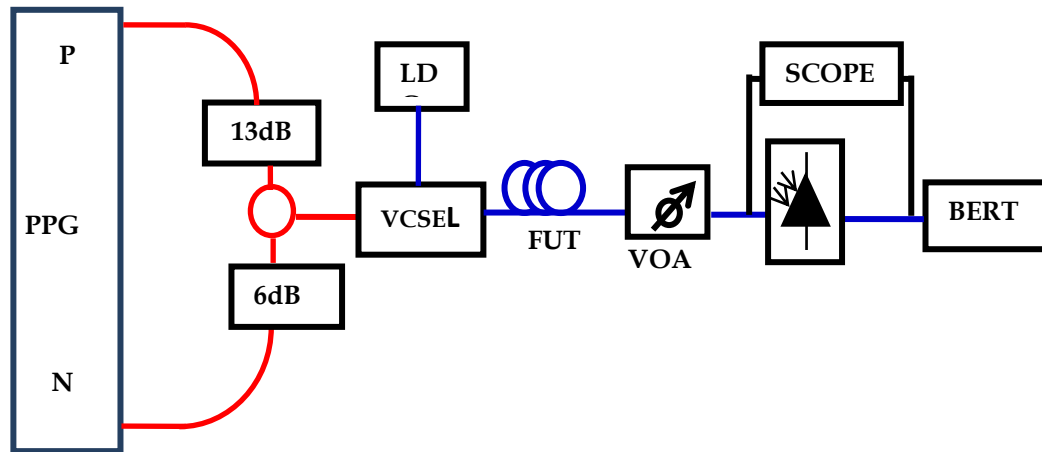


**Figure 3.8: 4-PAM Experimental modulation setup**

The data output from the two arms (P and N) of a PPG generates the PRBS ( $2^7-1$ ) at 10 Gbps. The data output from arm P is attenuated at 6 dBm and N attenuated at 13dBm this will guarantee the existence of signal with different power signals or amplitudes. Arm N which is attenuated at 13 dBm had their electrical data sequence delayed in time by an integer multiple of a bit period. After combining these data signals it directly modulates the VCSEL.

When the two signal are combined in the power combiner, the two signal interfere constructively and destructively to produce a four level data signal (4-PAM) that doubles the data rate to 20 Gbps. Before modulation and transmission of these signals, the multilevel transmitter codes two bits in one symbol. This signal is then transmitted through G.652 over a distance of 3.21 km.

At the receiver end a sampling oscilloscope was used. This is because of its ability to capture and store the received signal. Moreover, sampling oscilloscope has a very low noise floor and as a result of this, it produces one of the most accurate characterization of the 4-PAM. The captured eyes from the sampling oscilloscope were then transferred to an offline in order to extract its BER for analysis. The MATLAB algorithm makes use of the eyes from sampling oscilloscope as the input data.

4-PAM since it has four levels, threshold for each of the levels must be determined with their respective standard deviations computed. Three signal levels are practically applicable for 4-PAM format. Mean peak to peak voltage for each of the three eyes for level zero and one are calculated and their corresponding standard deviations determined. For each eye the threshold levels are then estimated based on their mean and standard deviations. The Q-factor is then calculated using the already obtained mean peak to peak voltages and their standard deviations. Finally, the actual BER is obtained as the cumulative error rate measurements done on each individual threshold values.

## CHAPTER FOUR

### RESULTS AND DISCUSSIONS

#### 4.1 State of Polarization in fibres

In the Figure 4.1, a WDM DFB laser was used to generate the signal which was then scrambled before monitoring the polarization states. The Poincare representation Figure 4.1 (a) and (b) shows comparative analysis of the polarization of a stable SMF and for the disturbed SMF respectively.

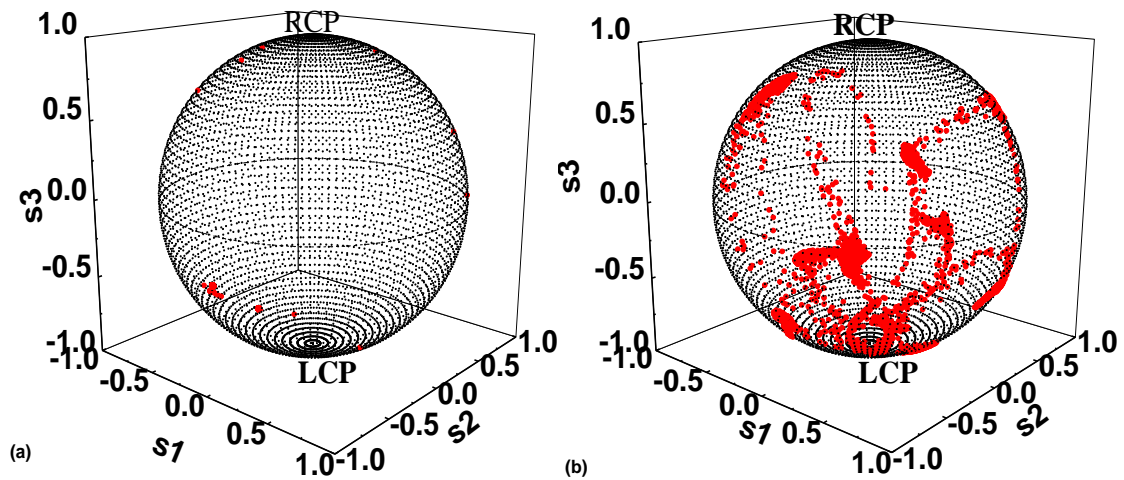


**Figure 4.1: Polarization states of (a) a stable SMF (b) disturbed SMF on a Poincare sphere.**

It's clearly noted that the magnitude of State of Polarization (SOP) indicated by the red markings on the Poincare sphere change more randomly when the fibre was under disturbed condition. The reduced fluctuations on the magnitude of SOP indicate a more stable signal transmitted in the fibre. The minimized SOP change is important in reducing polarization fluctuations of a signal transmitted in the fibre. Therefore, for improved stability in polarization dependent measurements, the fibre should be fixed to maintain a stable SOP.

The Poincare representation in Figure 4.2 shows a comparative analysis for the polarization of the PMF fibre under two different conditions. For Figure 4.2 (a) the fibre was kept in a stable condition and the polarization was then monitored. When the fibre was disturbed, the SOP monitored is as indicated in the Figure 4.2 (b) above.

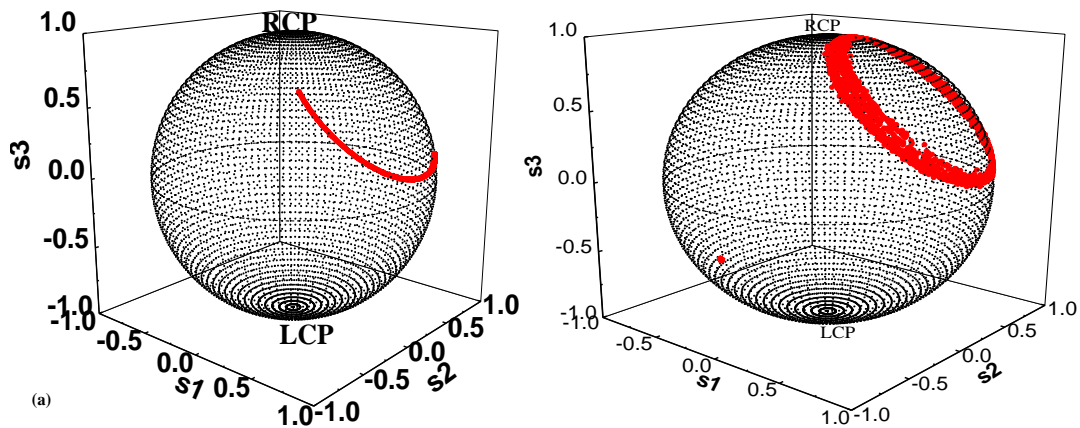


**Figure 4.2: SOP representation of (a) Stable PMF (b) disturbed PMF on a Poincare sphere**

It's clearly noted that under the two conditions, there is only a slight difference in the SOP. Therefore it's noted that the PMF stabilizes the polarization. From Figure 4.2 it's clearly seen that signal in a SMF in a stable mode (buried fibres) is more stable than a PMF under stable conditions.

#### **4.2 VCSEL biasing and tunability**

The biasing and tunability of the emission wavelength of 10 Gbps VCSEL were experimentally investigated and results presented in the Figure 4.3. Output power of the VCSEL was measured as the bias current was increased from 0 mA to 9.90 mA. As shown on the figure 4.3(a), the threshold current and peak current were observed at 0.92 mA and 6.5 mA respectively. As the bias current goes beyond 6.5 mA there is a dip in the



output power hence the VCSEL becomes very unstable and unpredictable. As a result, the best bias point to operate the VCSEL was at the middle of the linear region. During modulation, the VCSEL was biased at the middle of the linear region at 5.5 mA to provide a complete ON-OFF modulation swing. The bias current was restricted to 9.9 mA (without modulation) so as to avoid damaging the normal performance of the VCSEL.

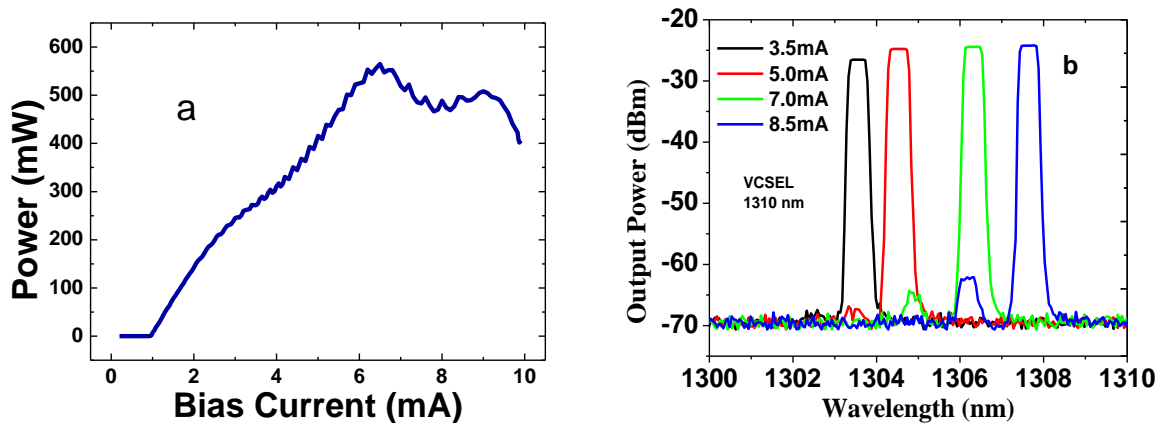


**Figure 4.3: (a) 1310 nm VCSEL Un-modulated bias characteristics (b) 1310 nm VCSEL tunability**

Tunability of the emission wavelength of VCSEL was done between 1303.48 nm to 1307.58 nm by varying the bias current from 3.5 mA to 8.5 mA. Biasing the VCSEL between 3.5-8.5 mA current, a 4.1 nm (512.01 GHz) wavelength range tunability obtained. This therefore can create 10 Gbps tunable channels within a 512.01 GHz bandwidth which can create 10 DWDM channels at a spacing of 50 GHz. In optical communication systems and flexible spectrum applications where wavelength tuning is required, VCSELs is a very important component.

### 4.3 VCSEL optimization for transmission

Figure 4.4 shows BER evaluation and their corresponding eye diagrams for B2B at different bias current levels done to determine the sensitivity levels of the receiver. VCSEL bias at 5.5 mA gave better BER performance than 4.5 mA, 7 mA and 8.5 mA since it gives better sensitivity.

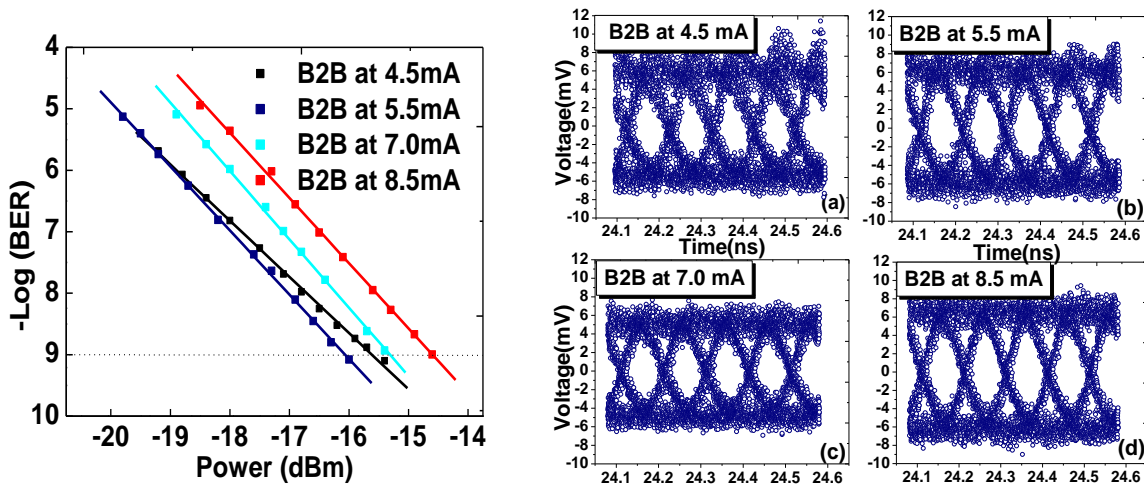


**Figure 4.4: BER curves and eye diagrams at different bias currents for 1550 nm VCSEL at (a) 4.5 mA (b) 5.5 mA (c) 7.0 mA (d) 8.5 mA**

At  $10^{-9}$  BER threshold level for a 5.5 mA bias current, the receiver sensitivity was seen to be -16.8 dBm while a 4.5 mA bias level had a -16.6 dBm. This provided a 0.2 dBm improvement in the PIN receiver sensitivity than when the VCSEL was biased at 4.5 mA. This is because at 5.5 mA it has a low BER with same receiver power hence the basis of biasing the subsequent transmissions. Having biased the VCSEL at 5.5 mA, this enables it to have a wide eye representing an error free modulation as shown in Figure 4.4 (b). When the eye was open, it shows that the receiver was able to distinguish between the '1's and '0's and therefore few errors were detected. However, the overshoots in the '1's level of the eye diagram was as a result of VCSEL chirping. An ideal turn on/off during

modulation is achieved when the laser is biased at the mid of the linear region. Under modulation and over-modulation of a laser results in electrical signal chirping. Biasing at 5.5 mA gave the widest eye as indicated in the eye diagrams above and best BER with least penalty.

#### 4.4 Effects of chromatic dispersion on transmission using 1550 nm VCSEL

To evaluate the performance of communication link the BER characteristics measurements were done for B2B and transmission over 17 km G.652 SMF as shown in Figure 4.5.

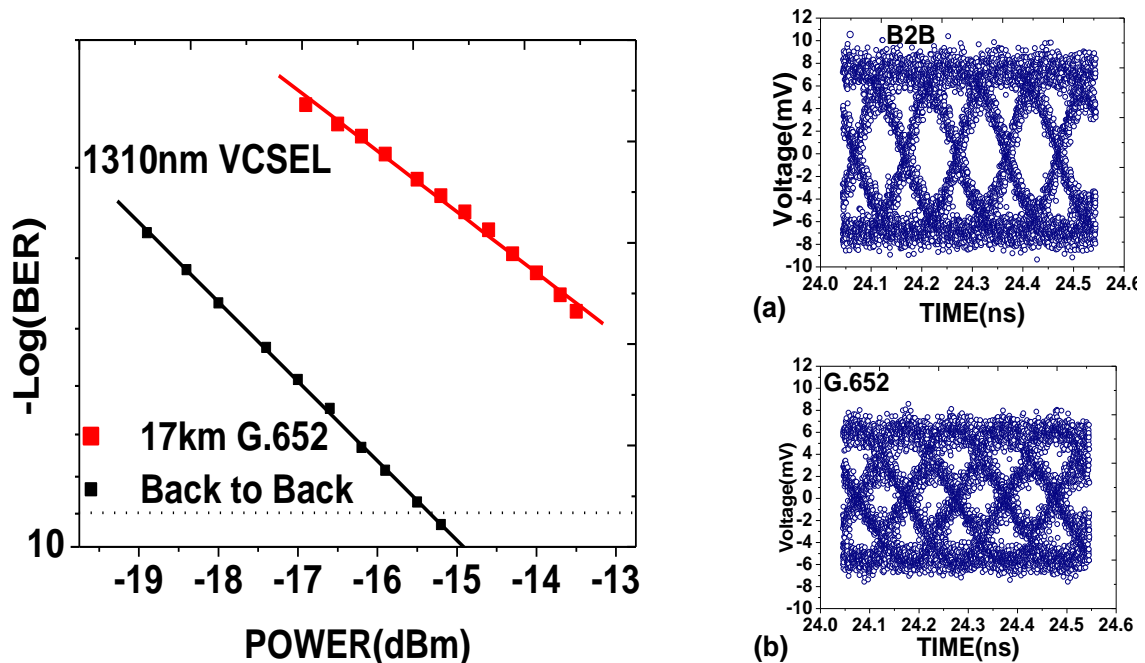


**Figure 4.5: Experimental demonstration of chromatic dispersion (a) eye diagram for B2B (b) eye diagram for 17 km G.652 fibre**

The receiver sensitivity for B2B were obtained as -15.32 dBm. However, for a Transmission over 17 km could not be able to cross at the minimum BER threshold of  $10^{-9}$  due to high chromatic dispersion in the fibre.

#### 4.5 Chromatic dispersion effects on the VCSEL based links

The optical communication system tolerance to the effects of dispersion were measured for 17 km of G.652 fibre and 24.69 km of G.655 fibre. The optical link was evaluated through BER measurements for B2B, 24.69 km and 17 km as indicated in Figure 4.6.

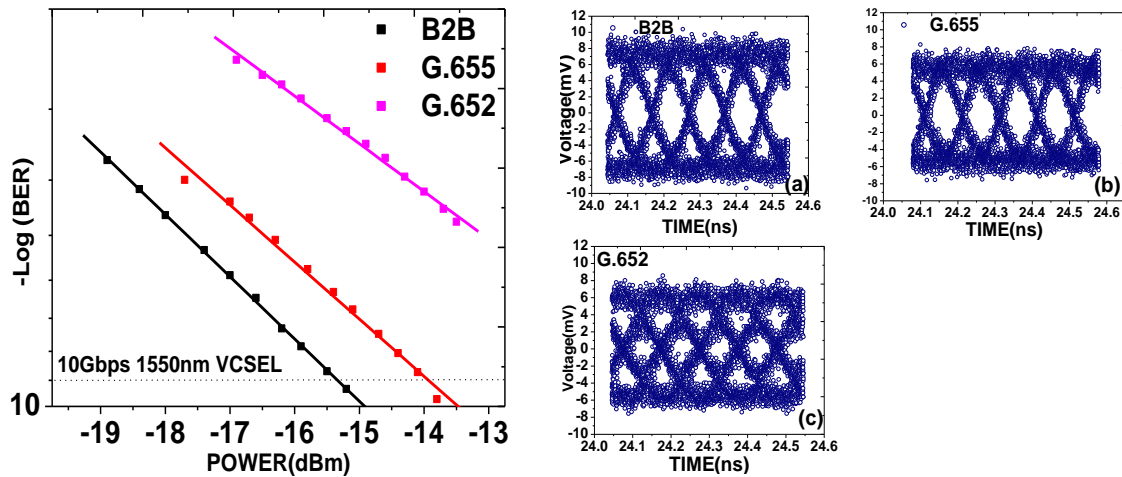


**Figure 4.6: Chromatic Dispersion effects on VCSEL based links (a) BER curves (b)**

**B2B (c) 24.69 km G.655 SMF-RS fibre (d) 17 km G.652 fibre**

The G.652 fibre used has low attenuation but has very high CD parameter of 17 ps/nm.km at 1550 nm as opposed to 0.35 ps/nm.km at 1310 nm. Use of G.652 fibre at 1550 nm despite having shorter length than G.655, it yielded non optimal performance due to effects of CD. Transmission over 24.69 km on ITU G.655 SMF-RS was achieved with 1.39 dBm penalty at BER of  $10^{-9}$  in comparison to B2B. An error free transmission was achieved for 24.69 km SMF-RS. This is attributed to the fact that the transmission distance is limited by high chromatic dispersion at 1550 nm transmission window for G.652. At 1550 nm wavelength G.652 fibres have very high CD of 17 ps/nm.km which resulted in increased number of error-bits received. This is because at 1550 nm window G.655 fibre has CD coefficient of 4.5 ps/nm/km as compared to a G.652 with CD

coefficient of 17 ps/nm/km and hence able to transit to a greater distance. The eye diagram for B2B, transmission over 24.9 km G.655 SMF-RS and 17 km G.652 SMF is similarly shown in the Figure 4.6 and shows the effect of dispersion on modulated signal. However, even at 24.69 km a sufficient open eye is still obtainable and at BER of  $10^{-9}$  is achieved with a power penalty of approximately 1.41 dBm in receiver sensitivity with respect to Back to Back.

#### 4.6 External Intensity Modulation and MZM biasing

Figure 4.7(a) indicates the output power in mW as a function of bias voltage. Figure 4.7(b) gives the output power in dBm as a function of bias voltage which indicates the extinction ratio between the high and low levels.

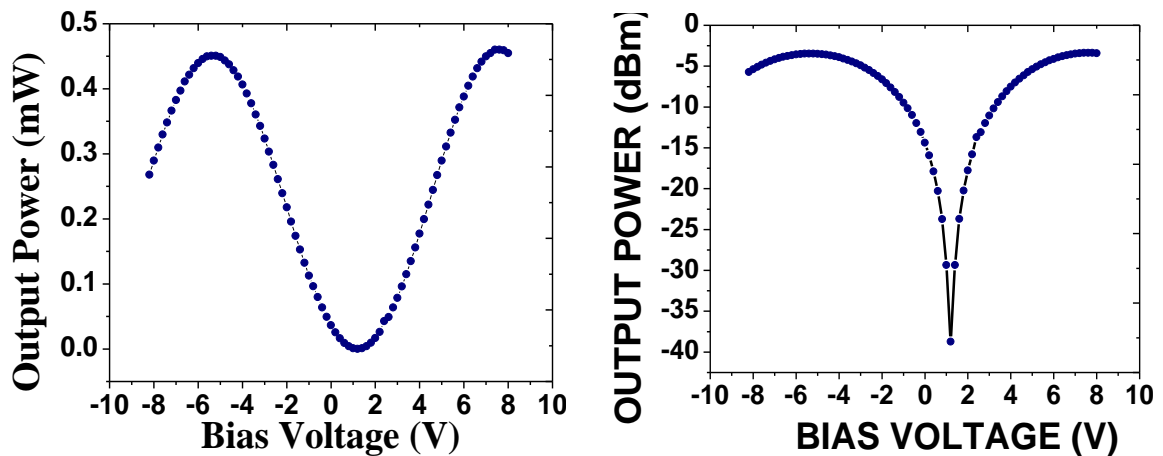


**Figure 4.7: Mach-Zender modulator biasing characteristics**

Many of the advanced modulation formats make use of MZMs. This is because they have good modulation performance and their possibility of independently modulating the phase and intensity of the optical field. (Agrawal, 2012; Peucheret & Fotonik, 2012b). These MZMs have different ways which can be driven in order to generate a variety of

modulation formats. The biasing and optimization of the Mach-Zender modulator is very important in order to get good signal quality.

#### 4.7 VCSEL transmission at different lengths

The Figure 4.8 shows the BER when three fibres of different lengths were used. For B2B the receiver sensitivity was observed at -18.858 dBm. When the signal was transmitted through a distance of 24.69 km over a SRS fibre the receiver sensitivity was observed to be -18.727 dBm which giving 0.131 dBm power penalty in comparison to the B2B. On changing the transmission reach to 49.42 km of SRS and RS fibre the receiver sensitivity of -18.467 dBm was attained with 0.391 dBm power penalty in comparison to B2B while at 74.91 km, -18.141 dBm receiver sensitivity was observed giving a power penalty of 0.717 dBm in comparison to B2B.

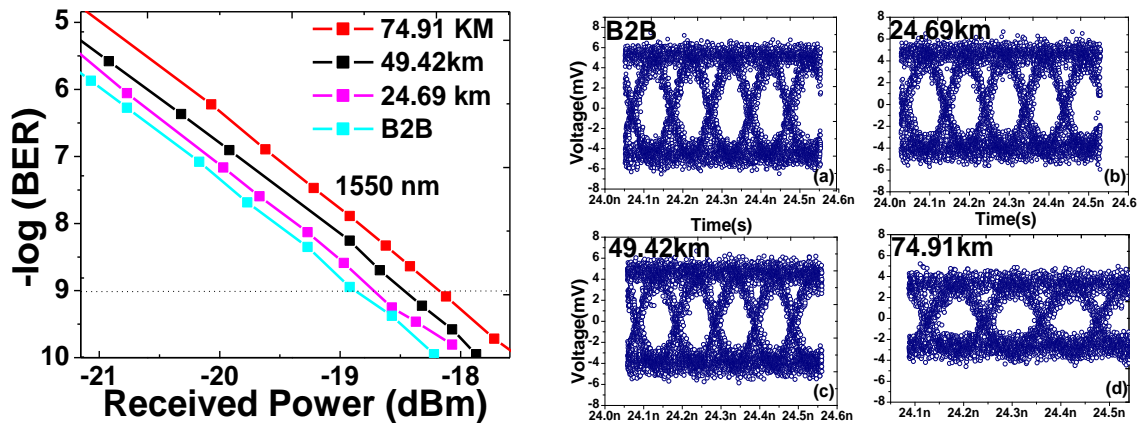


**Figure 4.8: BER graphs at different lengths for 10 Gbps**

This increase in power penalty as the distance increases signifies the power loss due to attenuation effects along the fibre link. The eye diagram for B2B, transmission over 24.69 km SRS, 49.42 km (24.69 km SRS +24.73 km RS) and 74.91 km (24.69 km SRS +24.73 km RS+25.49 km SRS) SMF in Figure 4.8 clearly shows the results of CD on the

signal. It was observed that increase in distance resulted in bit errors resulting in the overlapping of bits. The eye diagram closes its eyes for every transmission reach because of the effects of CD which degrades the quality of the signal. However, even at 74.91 km a sufficient open eye is still attainable at BER of  $10^{-9}$ . Increasing the distance to 74.91 km induces a penalty of 0.717 dBm in receiver sensitivity.

#### 4.8 Effects of changing the bit rate on VCSEL transmission

In Figure 4.9 the transmission penalty increases with increase in the bit rate and the fibre length. Increase in dispersion penalty with fibre length is caused by the cumulative effect of dispersion along the fibre link hence causing more penalties. Similarly, as bit rate increases, the bit cycle is reduced. Therefore, the effect of dispersion which was constant over fibre length on the bits led to more penalties as the distance increases. Figure 4.9 shows the eye diagrams for 8.5 Gbps and 10 Gbps respectively for a transmission distance of 74.91 km.

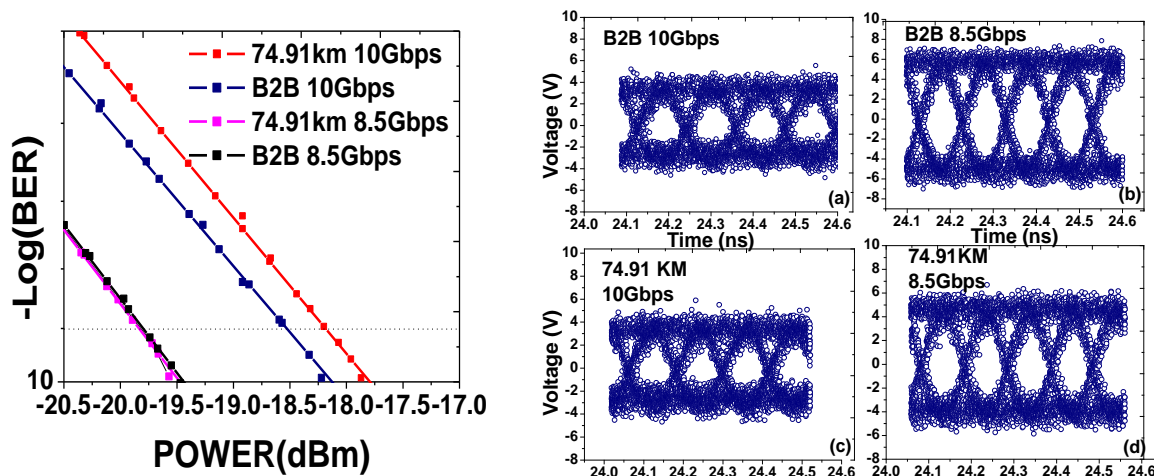


Figure 4.9: BER for B2B and 74.91 km transmission at 8.5 Gbps and 10 Gbps

At 8.5Gbps the eye is wide open indicating good signal clarity at 74.91 km. However, when the bit rate is increased to 10 Gbps it tends to close the eye. The reduction in the eye extinction ratio was attributed to the fact that when the bit rate increases the number of cycles increases per unit time and hence the system became more sensitive to the effects of chromatic dispersion. The transmission of 74.91 km at 8.5 Gbps has a very slight power penalty at BER of  $10^{-9}$  as compared to B2B. Sensitivity for B2B error free 8.5 Gbps signal was observed to be -19.9 dBm. By transmitting the signal over a 74.91 km the receiver error free sensitivity was -19.858 dBm and as a result a power penalty of 0.042 dBm was incurred.

#### **4.9 Transmission using Phase modulation (PM)**

In Figure 4.10 a delay line interferometer (DLI) was used in the setup. This setup is used to convert the phase keyed signal to an amplitude signal to meet the operational requirements of the receiver. The signal is first into two equal streams. In one of the arms, the signal is delayed by optical path difference equal to i-bit delay. When the two signals from the two arms are combined, they interfere constructively or destructively resulting in the intensity keyed signal. At the receiver, the signal was then collected in the form of eye diagrams for further offline processing. The optical communication link performance was then evaluated through BER measurements at different received powers. First, the eye diagrams were collected then taken to the DSP using MATLAB to extract the BER as illustrated in the Figure 4.10. Receiver sensitivity of -10.59 dBm was obtained as shown in Figure 4.10. The receiver sensitivity indicates the threshold power the receiver requires to demodulate the signal at BER of  $10^{-9}$ . BER values decreased at optical powers above the receiver sensitivity value giving error free transmission.



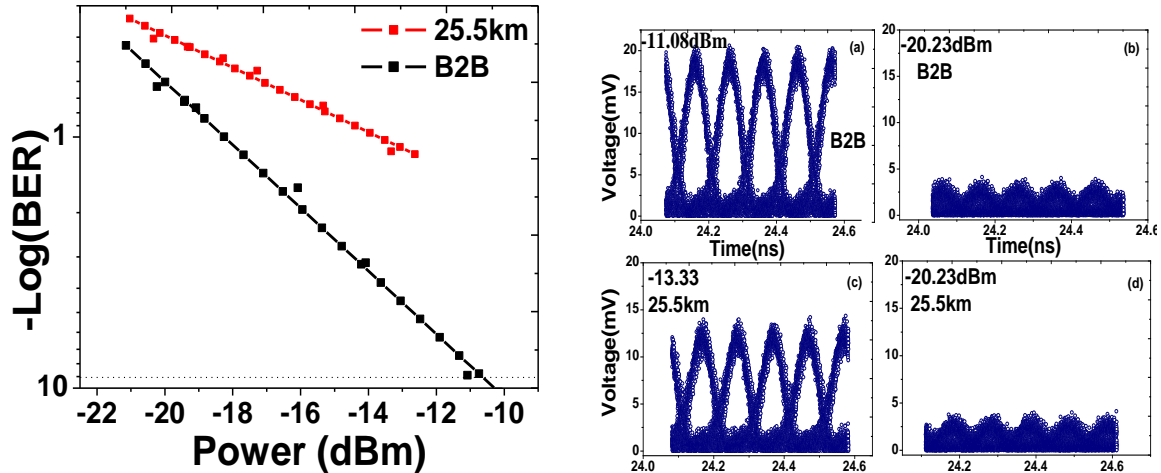


Figure 4.10: BER and eye diagrams for PSK format

When a 25.5 km G.655 SMF was introduced into the link, high optical power was required for the receiver to decode the signal properly. An error floor was obtained for 25.5 km and this was observed by the failure of the BER to cross the minimum threshold BER of  $10^{-9}$  as shown figure 4.10.

## 4.10 Pulse Amplitude Modulation (PAM)

### 4.10.1 Transmission using 2-Pulse Amplitude Modulation (2-PAM)

The Figure 4.11 shows the electrical signal waveform before and after combination.

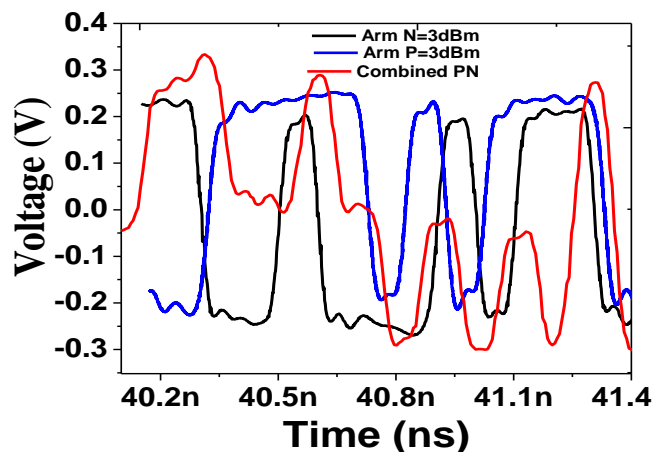
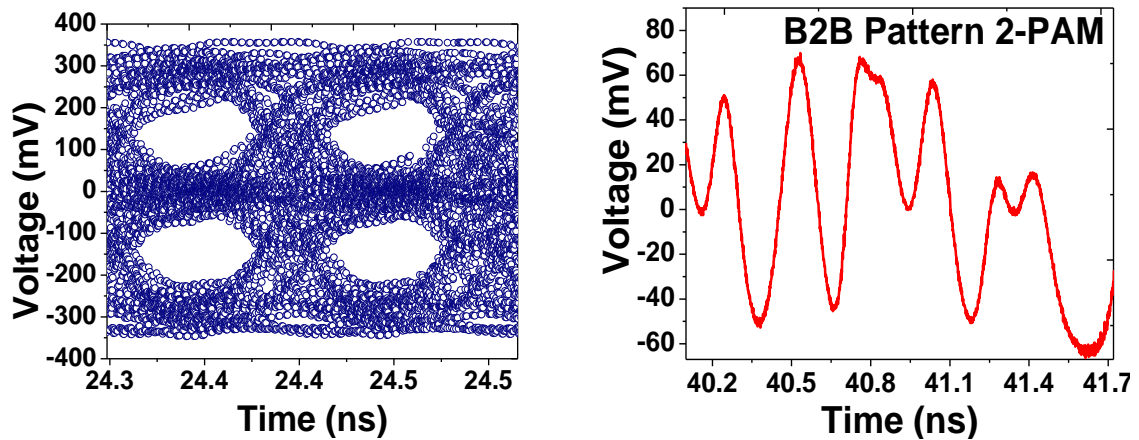


Figure 4.11: Arm P, Arm N and combined 2-PAM electrical signal

It is evidently clear that 2-PAM signal waveform is as a result of signal combination of the two signals (N and P). It has three levels as opposed to the conventional NRZ format that has two levels. The Figure 4.12(a) is a 2-PAM eye diagram and its corresponding signal pattern.



**Figure 4.12: B2B electrical 10 Gbps 2-PAM eye diagram and its optical signal waveform**

The Figure 4.13 shows the BER versus output power for a 1310 nm VCSEL for Back to back and G.652 transmission over 3.21 km. The eye opening is slightly bigger for B2B. When the signal had been transmitted through 3.21 km, distortion of the signal was visible through the eye diagrams due to inter-symbol interference. The eye diagrams from the sampling oscilloscope used to extract the BER using an offline MATLAB code.

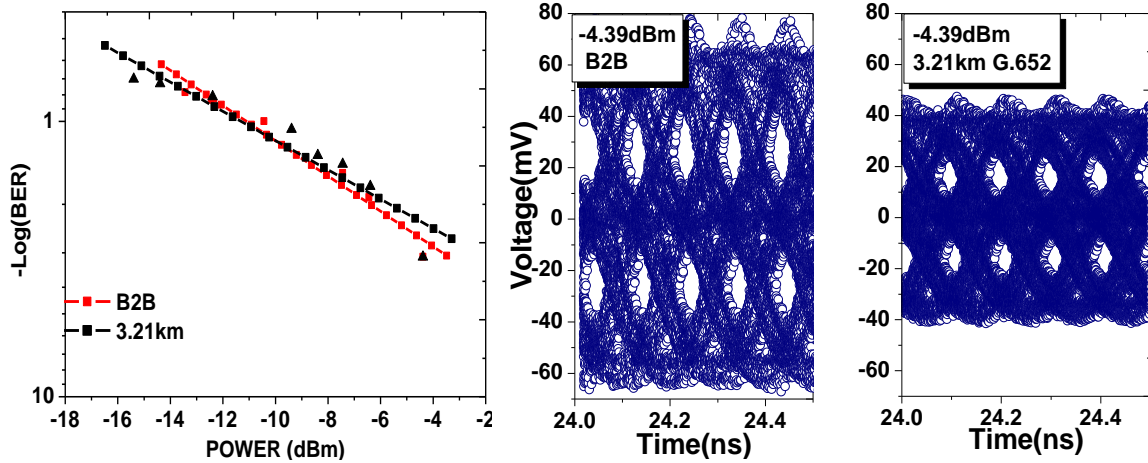


**Figure 4.13: BER Graph for B2B and transmission of 3.21 km and their eye diagrams for 2-PAM at 15 Gbps**

2-PAM format in Figure 4.13 indicates eyes are closing for every power decrement. The inability of 2-PAM to cross at BER of  $10^{-9}$  indicates that 2-PAM requires high optical power to demodulate the signal and thus results in higher power penalty as observed in the BER in figure 4.13 and this was indicated by the closure of the eye. The open eyes from figure 4.13 signify signal clarity. However, the eye height closes as the optical power decreases. This eye closure indicates signal loss due to attenuation effects within the fibre. The closure of the eye was attributed to the fact that a decrease in the input power increases the nonlinear effect in the fibre which is observed by the closure of the eye and therefore resulting in higher power penalty.

#### 4.10.2 Transmission using 4-Pulse Amplitude Modulation (4-PAM)

Figure 4.14 shows electrical data signal before and after combination of signal waveforms from the two arms. After mixing the two signals, through constructive and destructive interference four levels were created and each of the four levels comprises of two bits each (00; 01; 10 and 11).

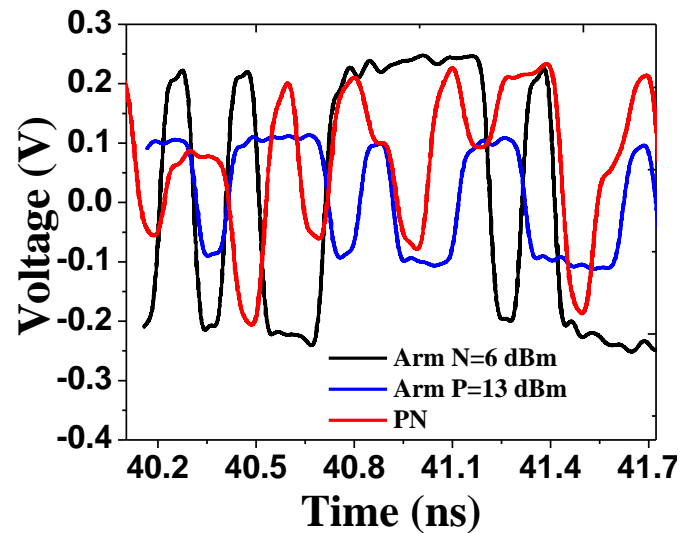


**Figure 4.14: P, N and combined 4-PAM electrical data signal**

The two electrical outputs were differentially attenuated to generate two binary data streams of different amplitudes. In one of the arm N it was attenuated to 6 dBm while arm P was attenuated to 13 dBm. The purpose of doubling the attenuation in one arm is to achieve a uniform eye opening.

The eye diagram for a 4-PAM showing the four levels with three eyes as indicated by Figure 4.15. each level of the four represents a combination of two bits (00, 01, 10, 11).

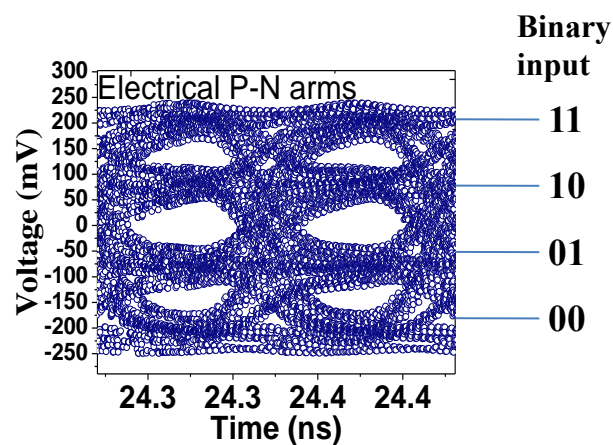


**Figure 4.15: B2B electrical 20 Gbps 4-PAM eye diagram**

Data rate is doubled because for every symbol period transmitted there are always two bits transmitted in parallel.

The Figure 4.16 shows the BER versus output power for a 1310 nm VCSEL at 20 Gbps for B2B and 3.21 km transmission on a G.652 fibre.

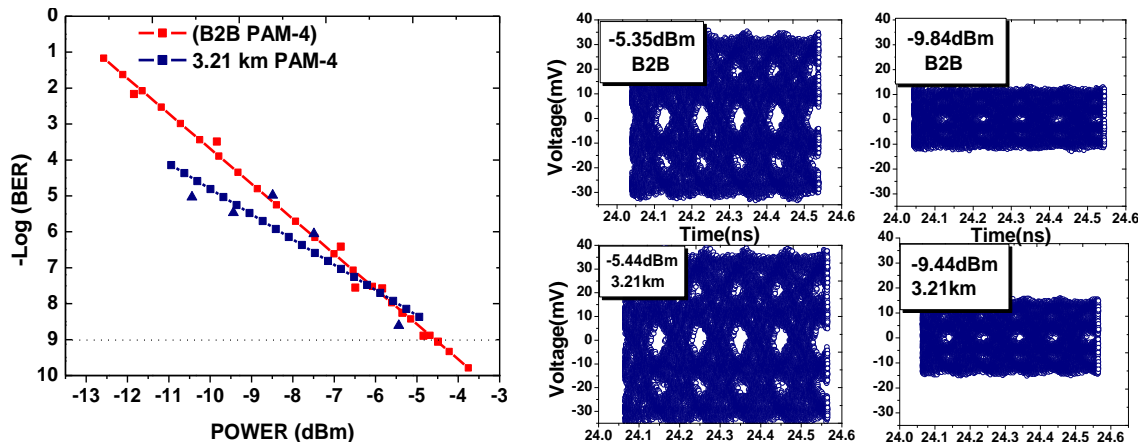


**Figure 4.16 : PAM-4 signal BER curve and eye diagrams**

The receiver sensitivity for B2B was observed to be approximately -4.542 dBm at BER threshold of  $10^{-9}$ . At 3.21 km transmission on a G.652 fibre sensitivity was observed at an approximately -3.817 dBm. This shows a power penalty of approximately 0.725 dBm. Eye diagrams for both B2B and 3.21 km are as displayed in figure 4.16 above. For B2B, the eye opening is slightly bigger. Degradation of the eye diagram after a transmission through 3.21 km is visible. This is attributed to the inter-symbol interference in addition to poor SNR. 4-PAM modulation format has the ability to double the data rate utilizing the same components. In 4-PAM modulation format the eye opening decreases with power decrement. The extracted BER shows that 4-PAM has a lower receiver sensitivity as compared to NRZ but this is however mitigated by its high throughput.

#### 4.11 Comparison of transmission penalties for IM, Phase modulation, 2-PAM and 4-PAM

The figure 4.17 BER graphs showing different modulation formats. Analysis and comparison of four modulation formats were done. In NRZ binary modulation format the signal is switched between two levels '0' and '1'. In PSK format the modulation is done on the phase while keeping the amplitude and the frequency of the optical carrier constant.

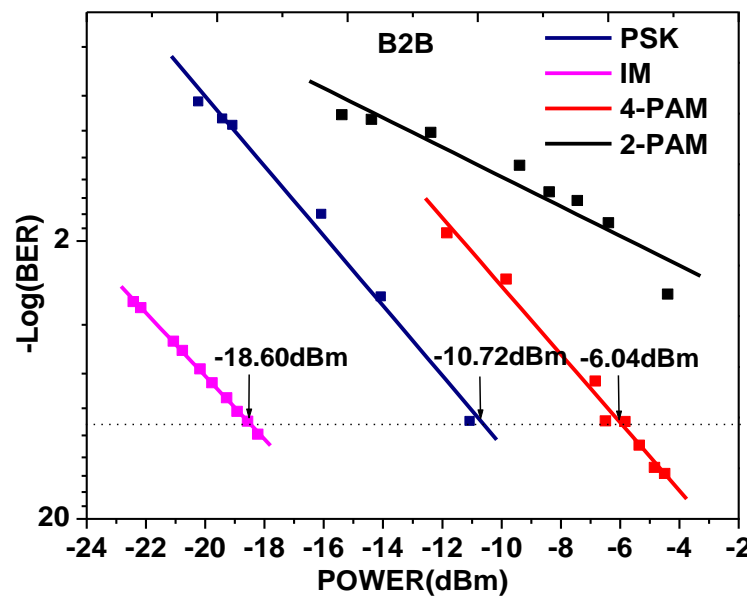


**Figure 4.17: BER curves for IM, Phase modulation, 2-PAM and 4-PAM**

NRZ and PSK signals was measured to be -18.60 dBm and -10.72 dBm respectively. NRZ gave a better receiver sensitivity of -7.88 dBm in comparison to PSK. The higher penalty in the 4-PAM compared to NRZ and PSK was as a result of modulation of the additional bits which were at the same modulation depths this resulted in the need for a more sensitive receiver which can be able to demodulate the two bits per symbol. From this, it's evident that IM gave a better receiver sensitivity of 7.88 dBm than PSK

modulation, 2-PAM and 4-PAM format. However, 4-PAM despite having higher receiver sensitivity, it's compensated by its high data throughput.

#### 4.12 Comparison of DFB laser and VCSEL

The Figure 4.18 shows BER graph for VCSEL and DFB Lasers. The performance of the two lasers were analyzed and compared based on their receiver sensitivity.

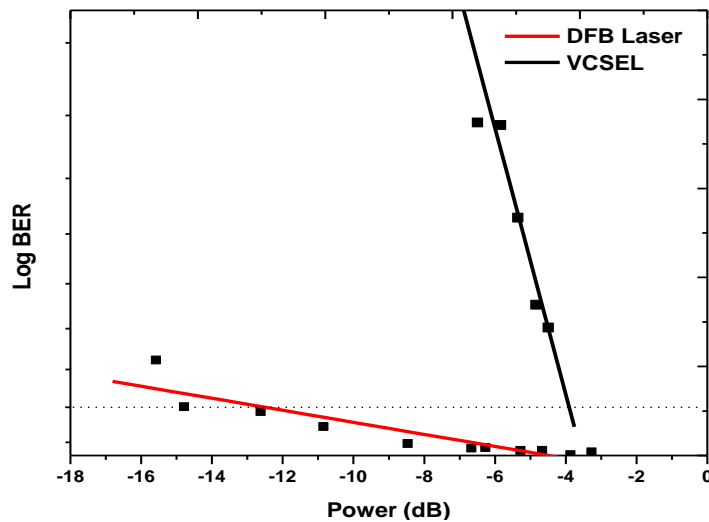


**Figure 4.18: BER curves for DFB and VCSEL**

VCSEL laser provides low power consumption and has a wider temperature range than DFB. VCSEL being a low power laser makes it the best choice for direct modulation. This is observed in Figure 4.18 with a receiver sensitivity of -12.6 dBm as compared to DFB laser with sensitivity of -3.86 dBm giving a penalty of 8.74 dBm.

## CHAPTER FIVE

### CONCLUSIONS AND RECOMMENDATIONS

#### 5.1 CONCLUSION

Optical communication system tolerance to the effects of dispersion was investigated for G.652 and G.655 fibres. at 1550 nm window the G.652 fibre showed high CD which yielded non-optimal performance leading to increased number of error-bits received.

Performance of the four modulation formats were also analyzed and compared in relation to their receiver sensitivity. The BER evaluation performance was computed using the designed DSP aided receiver. NRZ, PSK, 2-PAM and 4-PAM were investigated with respect to their receiver sensitivity. NRZ gave the best receiver sensitivity followed by PSK, 4-PAM and 2-PAM respectively. However, a lot of power is required by 2-PAM to demodulate and therefore unable to achieve the bit error rate threshold of  $10^{-9}$ . A cost effective 20 Gbps multilevel system on the other hand was successfully designed by combining two electrical data streams at 10 Gbps, as opposed to using a more expensive single optical transmitter that operates at the same speed. A 20 Gbps transmission link was demonstrated from  $2 \times 10$  Gbps transmitter. The 4-PAM signal was transmitted successfully through 3.21 km distance on a G.652 fibre. This format can be utilized in the already laid communication link by doing a small modification of the transmitter alone. The developed format can simultaneously transmit two bits per symbol per wavelength hence increasing the transmission rate while utilizing the same channel bandwidth.



Comparison between DFB and VCSEL lasers based on their sensitivity were also done. VCSEL is a specialized laser diode with improved efficiency, provides low power consumption and wider temperature range than DFB. However, it's a low power laser, making it the best choice for direct modulation and hence suitable for access network. This is observed from its low receiver sensitivity in comparison to a DFB laser. DFB on the other hand is a high power laser making it suitable for long distance transmission and hence high receiver sensitivity.

A DSP algorithm was developed making use of probability Density Function (PDF) and Quality factor (Q). This technology helps to evaluate and monitor the performance of advanced modulation format when relevant hardware is absent. The offline signal analyzer and the multilevel transmitter developed and experimentally tested are technologies that can assist reduce the growing urge for transmission speeds. The developed DSP algorithm can be used for any advanced modulation format leading to a cost effective way of evaluating performance of high speed communication link.

The offline DSP receiver with its ability to be reconfigured is a suitable candidate for use in optical communication industries and in research institution. Further reduction in the implementation of this scheme is achieved also by the ability of making use of a single photodiode in demodulation of these multilevel signals. This modulation format can achieve even higher data rates when integrated in a DWDM system. These results obtained in this experimental investigation will give an optical network designer a well informed decision on the modulation format suitable for system upgrade.

## 5.2 RECOMMENDATIONS

- 4-PAM format suits access networks due to its high carrying capacity, efficiency and reliability.
  
- G.655 fibre is better used in access networks than G.652

## REFERENCES

- Abdullah M. & Talib R. (2012). Multilevel signal analyzer tool for optical communication system. *International Journal of Electrical and Computer Engineering*, 2(4), 529.
- Agalliu R. & Lucki M. (2014). Benefits and Limits of Modulation Formats for Optical Communications. *Advances in Electrical and Electronic Engineering*, 12(2), 160.
- Agrawal G. P. (2002). Nonlinear optics: *IEEE*.
- Agrawal G. P. (2012). *Fibre-optic communication systems* (Vol. 222): 4th edition, John Wiley & Sons, Hoboken, New Jersey.
- Al-Dwairi M. (2013). Evaluation of Multilevel Modulation Formats for 100Gbps Transmission with Direct Detection. World Academy of Science, Engineering and Technology, *International Journal of Electrical, Computer, Energetic, Electronic and Communication Engineering*, 7, 1060-1066.
- Bo Z., Xiaoxue Z., Christin L., Parekh D., Hoffmann W., Wu M. C, Amann M. C., Chang-Hosnain C. J. and Willner A. E. (2008). Adjustable Chirp Injection - Locked 1.55 $\mu\text{m}$  VCSELs for enhanced chromatic dispersion compensation at 10Gbps, *optical fibre communication/ National fibre optic engineers conference, OFC/NFOEC,2008*, pp. 1-3
- Born M. and Wolf E. (1999), *Principles of Optics. Electromagnetic Theory of Propagation, Interference and Diffraction of Light*, (7th ed.), Cambridge University Press, UK, ISBN-13 : 978-0521642224.
- Chagnon M., et al.,(2014). Experimental study of 112 Gb/s short reach transmission employing PAM formats and SiP intensity modulator at 1.3  $\mu\text{m}$ . *Optics express*,22(17): p. 21018-21036.
- Dennis M. L., Hayee M. I., Mahon C., Pedersen B., Ramanujam N. & Shieh W. (2003). Method and system for dispersion maps and enhanced distributed gain effect in long haul telecommunications: Google Patents.
- Dutton H. J. (1998). *Understanding optical communications*: Prentice Hall PTR Upper Saddle River, NJ, ISBN-13 : 978-0130201416
- Elahmadi S., Srinath M. D., Rajan D. & Haberrman R. (2009). Channel capacity and modeling of optical fibre communications. Paper presented at the Wireless and Optical Communications Networks. WOCN'09. *IFIP International Conference*. : <https://www.researchgate.net/publication/224483641>

- Gatto A., Boletti A., Boffi P., Neumeyr C., Ortsiefer M., Rönneberg E. & Martinelli M. (2009). 1.3-m VCSEL Transmission Performance up to 12.5 Gb/s for Metro Access Networks. *IEEE Photonics Technology Letters*, 21(12).
- Gibbon T. B., Prince K., Pham T. T., Tatarczak A., Neumeyr C., Ronneberg E. and Ortsiefer M. (2011). VCSEL transmission at 10Gbps for 20Km single mode fibre WDM-PON without dispersion compensation or injection locking, *optical fibre technology*, 17(2011), 41-45.
- Haris M. (2008). Advanced modulation formats for high-bit-rate optical networks. Georgia Institute of Technology, <http://hdl.handle.net/1853/24811>
- Hoshida T., Vassilieva O., Yamada K., Choudhary S., Pecqueur R., & Kuwahara H. (2002). Optimal 40 Gb/s modulation formats for spectrally efficient long-haul DWDM systems. *Journal of lightwave technology*, 20(12), 1989-1996.
- Isoe G., et al. (2017) A high capacity data centre network: simultaneous 4-PAM data at 20 Gbps and 2 GHz phase modulated RF clock signal over a single VCSEL carrier. *Journal of Modern Optics*, 64(21): p. 2336-2344.
- Isoe G., et al. (2017). Capacity upgrade in short-reach optical fibre networks: simultaneous 4-PAM 20 Gbps data and polarization-modulated PPS clock signal using a single VCSEL carrier. *Journal of Modern Optics*, 64(20): p. 2245-2254
- Ibrahim S. K. (2007). *Study of Multilevel Modulation Formats for High Speed Digital Optical Communication Systems*, Ph.D. Dissertation, University of Paderborn.
- Iga K. (2000). Surface-emitting laser-its birth and generation of new optoelectronics field. *IEEE Journal of Selected Topics in Quantum Electronics*, 6(6), 1201-1215.
- Jensen J. B., Olmeido M. I., & Monroy I. T. (2013). Modulation formats for beyond-100Gbps Ethernet optical links-a review of research. *Asia Communications and Photonics Conference*, Beijing China, 12-15 November 2013, ISBN: 978-1-55752-989-3
- Jopson B., & Gnauck A. (1995). Dispersion compensation for optical fibre systems. *IEEE communications magazine*, 33(6), 96-102.
- Ju Han L., You Min C., Young-Geun, H., Sang Hyuck, K., Haeyang, C., & Sang Bae, L. (2005). Dispersion-compensating Raman/EDFA hybrid amplifier recycling residual Raman pump for efficiency enhancement. *IEEE Photonics Technology Letters*, 17(1), 43-45.
- Kaminow I., Li T., & Willner A. E. (2010). *Optical fibre telecommunications VB: systems and networks*: Elsevier, ISBN: 0-12-395172-0.

- Karinou F., Prodaniuc C., Stojanovic N., Ortsiefer M., Daly A., Hohenleitner R., Neumeyr C. (2015). Directly PAM-4 Modulated 1530-nm VCSEL Enabling 56 Gb/s/ $\lambda$  Data-Center Interconnects. *IEEE Photonics Technology Letters*, 27(17), 1872-1875.
- Karinou F., Rodes R., Prince K., Roudas I., & Monroy I. T. (2013). IM/DD vs. 4-PAM using a 1550-nm VCSEL over short-range SMF/MMF links for optical interconnects. *Optical Fibre Communication Conference and Exposition and the National Fibre Optic Engineers Conference (OFC/NFOEC)*, Anaheim, California United States, 17-21 March 2013, ISBN: 978-1-55752-962-6
- Keiser G. (2003). *Optical fibre communications*. Wiley Encyclopedia of Telecommunications.
- Keiser G. (2010). *Optical fibre communications*: McGraw-Hill, 4th Edition, ISBN 13: 978-0073380711
- Kent D. C., Dominic F. S., Ansas M. K., Meng P. T., Joshua D.S., Paul O. L., James J. R. Jr. and Aaron J. D. (2012). Single Mode Photonic Crystal Vertical Cavity Surface Emitting Lasers, Hindawi Publishing Corporation, *Advances in Optical Technologies*, doi:10.1155/2012/280920
- Kipnoo E. K., Kourouma H., Chabata T. V., Gamatham R. R. G., Leitch A. W. R. and Gibbon T. B. (2013). Optimizing VCSEL transmission for longer reach in optical access networks, *16<sup>th</sup> South African Telecommunication Networks and Applications Conference*, Spier, Stellenbosh, Western Cape, South Africa, pp 27-30
- Koizumi Y., Toyoda K., Yoshida M., & Nakazawa M. (2012). 1024 QAM (60 Gbit/s) single-carrier coherent optical transmission over 150 km. *Optics express*, 20(11), 12508-12514.
- Kondow M., Kitatani T., Nakahara K., & Tanaka T. (2000). Temperature dependence of lasing wavelength in a GaInNAs laser diode. *IEEE Photonics Technology Letters*, 12(7), 777-779.
- Koyama F. (2006). Recent advances of VCSEL photonics. *Journal of lightwave technology*, 24(12), 4502-4513.
- Krehlik P. (2006). Characterization of semiconductor laser frequency chirp based on signal distortion in dispersive optical fibre. *Opto-electronics review*, 14(2), 119-124.
- Kuchta D. M. (2016). Directly modulated VCSELs at  $\geq 50$  Gb/s for short reach data communications. *IEEE Optical Interconnects Conference (OI)*, 9-11 May 2016, San Diego, CA, USA.

- Lach E., & Idler W. (2011). Modulation formats for 100G and beyond. *Optical Fibre Technology*, 17(5), 377-386.
- Lauermann M., Palmer R., Koeber S., Schindler P., Korn D., Wahlbrink T., Dalton L. (2014). Low-power silicon-organic hybrid (SOH) modulators for advanced modulation formats. *Optics express*, 22(24), 29927-29936.
- Li X., Chen, X., Goldfarb G., Mateo E., Kim I., Yaman F., & Li G. (2008). Electronic post-compensation of WDM transmission impairments using coherent detection and digital signal processing. *Optics express*, 16(2), 880-888.
- Li X., Mardling, R., & Armstrong J. (2007). Channel capacity of IM/DD optical communication systems and of ACO-OFDM. Paper presented at the Communications, 2007. ICC'07. *IEEE International Conference*, 24-28 June 2007, Glasgow, UK.
- Lin C.-K., Bour D. P., Zhu J., Perez W. H., Leary M. H., Tandon A., Tan M. R. (2003). High temperature continuous-wave operation of 1.3-and 1.55- $\mu\text{m}$  VCSELs with InP/air-gap DBRs. *IEEE Journal of Selected Topics in Quantum Electronics*, 9(5), 1415-1421.
- Lin C., Cohen L., & Kogelnik H. (1980). Optical-pulse equalization of low-dispersion transmission in single-mode fibres in the 1.3–1.7- $\mu\text{m}$  spectral region. *Optics letters*, 5(11), 476-478.
- Lin Q., Painter O. J., & Agrawal G. P. (2007). Nonlinear optical phenomena in silicon waveguides: modeling and applications. *Optics express*, 15(25), 16604-16644.
- Lopez R. R. (2013). Vertical-Cavity Surface-Emitting Lasers: Advanced Modulation Formats and Coherent Detection, Kgs. Lyngby, *Technical University of Denmark*.
- Lyubomirsky I. (2005). Advanced modulation Formats for Ultra-Dense Wavelength Division Multiplexing. *International Research Journal of Engineering and Technology (IRJET)*, Volume: 04 (Issue: 06).
- Meltenisov M., & Matukhin A. (2016). Analytical model of chromatic dispersion effect in the time domain. *Advanced Communication Technology (ICACT)*, 2016 18th International Conference, 31 Jan.-3 Feb. 2016, Pyeongchang, South Korea.
- Mereuta A., Syrbu A., Iakovlev V., Rudra A., Caliman A., Suruceanu G., Kapon E. (2004). 1.5  $\mu\text{m}$  VCSEL structure optimization for high-power and high-temperature operation. *Journal of Crystal growth*, 272(1), 520-525.

- Messerschmitt D. G. (1999). *Understanding Networked Applications*. University of California, Morgan Kaufmann Publishers Inc., San Francisco, CA, United States, ISBN:978-1-55860-537-4
- Mohapatra S., Bhojray R., & Mandal S. (2013). Analog and Digital Modulation Formats of Optical Fibre Communication within and Beyond 100 Gb/S: A Comparative Overview. *International Journal of Electronics and Communication Engineering & Technology (IJECEET)*, 4(2), 198-216.
- Mohapatra S. K., Choudhury R. R., Bhojray R., & Das P. (2014). Performance Analysis and Monitoring of Various Advanced Digital Modulation and Multiplexing Techniques of FOC Within and Beyond 400 Gb/S. *International Journal of Computer Networks & Communications*, 6(2), 159.
- Nakazawa M., Okamoto S., Omiya T., Kasai K., & Yoshida M. (2010). 256-QAM (64 Gb/s) coherent optical transmission over 160 km with an optical bandwidth of 5.4 GHz. *IEEE Photonics Technology Letters*, 22(3), 185-187.
- Nuyts R. J., Park Y. K., & Gallion P. (1997). Dispersion equalization of a 10 Gb/s repeatered transmission system using dispersion compensating fibres. *Journal of lightwave technology*, 15(1), 31-42.
- O.F.S. Furukawa, (2017). Understanding fibre optics-Attenuation. <https://www.fibre.optic-catalog.ofsoptics.com.pdf>, Accessed 30Th October, 2018
- Okoshi, T. (1981). Single-polarization single-mode optical fibres. *IEEE journal of quantum electronics*, 17(6), 879-884.
- Petermann K. (1988). *Laser diode modulation and noise*, Kluwer Academic, Dordrecht.
- Peucheret C., & Fotonik D. (2012a). Generation and detection of optical modulation formats. *Department of Photonics Engineering Technical University of Denmark*.
- Peucheret, C., & Fotonik, D. (2012b). Generation and detection of optical modulation formats. *Dept. of Photonics Eng, Technical University of Denmark*.
- Pham T.-T., & Monroy I. T. (2012). Data transmission techniques for short-range optical fibre and wireless communication links, *Technical University of Denmark, Kgs. Lyngby, Denmark*.
- Princeton Optronics, <https://www.newmetals.co.jp/pdf/234.pdf>, Accessed 30Th October, 2018
- Ratio O.S.-t.-N., (2008). The Q-factor in Fiber-Optic Communication Systems. Maxim application note HFAN, 9(2).

- Snitzer E., & Osterberg H. (1961). Observed dielectric waveguide modes in the visible spectrum. *JOSA*, 51(5), 499-505.
- Stokes G. G. (1852). On the change of refrangibility of light. *Philosophical transactions of the Royal Society of London*, 142, 463-562.
- Ten S., & Edwards M. (2006). An Introduction to the Fundamentals of PMD in Fibres. white paper, available from: < [www.corning.com/WorkArea/downloadasset.aspx](http://www.corning.com/WorkArea/downloadasset.aspx), 6th Jan, 2021.
- Thorlabs (2017) <https://www.thorlabs.com/DCF38.pdf>, Accessed 30th October, 2018.
- Tricker R. (2002). Optoelectronics and fibre optic technology: *Elsevier*, ISBN: 9780080513263.
- Vodhanel R. S., Elrefaie A. F., Iqbal M., Wagner R. E., Gimlett J. L., & Tsuji S. (1990). Performance of directly modulated DFB lasers in 10-Gb/s ASK, FSK, and DPSK lightwave systems. *Journal of lightwave technology*, 8(9), 1379-1386.
- Winzer P. J., & Essiambre R.-J. (2006). Advanced optical modulation formats. *Proceedings of the IEEE*, 94(5), 952-985.
- Wuth T., Kaiser W., & Rosenkranz W. (2001). Impact of self-phase modulation on bandwidth efficient modulation formats. *Optical Fibre Communication Conference and Exhibit*, Anaheim, California United States, 17 March 2001, ISBN: 1-55752-654-0
- Yamamoto T. (2012). High-speed directly modulated lasers. *Optical Fibre Communication Conference and Exposition (OFC/NFOEC), and the National Fibre Optic Engineers Conference*, Los Angeles, California United States, 4-8 March 2012, ISBN: 978-1-55752-938-1
- Zhang X. (2012). Digital Signal Processing for Optical Coherent Communication Systems: DTU Fotonik, *Department of Photonics Engineering*, Technical University of Denmark.



## APPENDICES

### APPENDIX I: MATLAB ALGORITHM

```

clear all
filename='data-74.txt'
dataArray=importdata(filename);
% plot(dataArray, 'r o');
% xlabel('Time');
% ylabel('Voltage');
eye_1=[];eye_2=[];eye_3=[];eye_4=[];
y=prctile(dataArray,33);
x=prctile(dataArray,66)
for i=1:1:48382;%number of data points of the selected part of the most open eye;
    if dataArray(i,1)<0.9843750000000000%to separate positives only, column 1 (COPY
AND PASTE THE EYE THRESHOLD)
        y0=dataArray(i,1);%select column 1
        eye_1=cat(1,eye_1,y0);%Name of worksheet with values on column 1
    else
        y4=dataArray(i,1);%to separate negatives only
        eye_4=cat(1,eye_4,y4);%Name of worksheet with values on column 1
    if dataArray(i,1)>1.9765625000000000
        s1=dataArray(i,1);
        eye_2=cat(1,eye_2,s1);
    else
        y2=dataArray(i,1);
        eye_3=cat(1,eye_3,y2);
    end
    end
end
end
level_00=[];level_01=[]
eye_threshold1=mean(eye_1)
format long
for i=1:1:15876;
    if eye_1(i,1)>0.4882812500000000;
        s2=eye_1(i,1);
        level_01=cat(1,level_01,s2);
    else
        s1=eye_1(i,1);
        level_00=cat(1,level_00,s1);%Name of worksheet with values on column 1
    end
end
end
MEAN_level_1=mean(level_01);
MEAN_level_0=mean(level_00);

```

```
sigma00=0.0999660297;  
sigma01=0.0809214437;  
x=MEAN_level_1-MEAN_level_0;  
t=sigma00+sigma01;  
Q=x./t  
X=1-(erf(Q*(2^-0.5)));  
BER = 0.5*X  
BER_VALUE=-log10(BER)
```

## APPENDIX II: SIMILARITY REPORT

Turnitin https://www.turnitin.com/newreport\_classic.asp?lang=en\_us&o...


---

## Turnitin Originality Report

Processed on: 15-Jan-2021 14:31 EAT  
 ID: 1488007626  
 Word Count: 18485  
 Submitted: 1

SC/PHD/P/035/12 By Yegon  
 Geoffrey Kipkoeh

Document Viewer



---

Similarity Index

# 17%

**Similarity by Source**

Internet Sources:	11%
Publications:	10%
Student Papers:	7%

include quoted   
  include bibliography   
  excluding matches < 5 words   
 mode:

quickview (classic) report   
 Change mode   
 print   
 refresh   
 download

---

<p>&lt;1% match (publications)  <u>Sanjeev Kumar Raghuwanshi, Akash Srivastav. "Review of Microwave Photonics Technique to Generate the Microwave Signal by Using Photonics Technology", Journal of Optical Communications, 2017</u> <span style="float: right;">✖</span></p>
<p>&lt;1% match (student papers from 09-Dec-2014)            Submitted to Institute of Technology, Nirma University on 2014-12-09 <span style="float: right;">✖</span></p>
<p>&lt;1% match (Internet from 16-Jun-2019)  <a href="http://dev2.4science.net">http://dev2.4science.net</a> <span style="float: right;">✖</span></p>
<p>&lt;1% match (Internet from 17-Sep-2018)  <a href="https://www.export.gov/article?id=Kenya-telecommunications-equipment">https://www.export.gov/article?id=Kenya-telecommunications-equipment</a> <span style="float: right;">✖</span></p>
<p>&lt;1% match (publications)  <u>F. Le Roy-Brehonnet, B. Le Jeune. "Utilization of Mueller matrix formalism to obtain optical targets depolarization and polarization properties", Progress in Quantum Electronics, 1997</u> <span style="float: right;">✖</span></p>
<p>&lt;1% match (Internet from 12-Feb-2011)  <a href="http://www.ausoptic.com.au">http://www.ausoptic.com.au</a> <span style="float: right;">✖</span></p>
<p>&lt;1% match (student papers from 26-May-2017)            Submitted to All Saints Anglican School on 2017-05-26 <span style="float: right;">✖</span></p>
<p>&lt;1% match (Internet from 30-Jun-2020)  <a href="http://www.opticsphotonics.org">http://www.opticsphotonics.org</a> <span style="float: right;">✖</span></p>
<p>&lt;1% match (publications)  <u>Govind P. Agrawal. "Fiber Optic Raman Amplifiers", Elsevier BV, 2006</u> <span style="float: right;">✖</span></p>

1 of 51

1/18/2021, 9:59 AM